C.P. No. 1334

C.P. No. 1334

PROCUREMENT EXECUTIVE, MINISTRY OF DEFENCE

AERONAUTICAL RESEARCH COUNCIL

CURRENT PAPERS

Interference Problems on Wing-Fuselage Combinations Part IV The Design Problem for a Lifting Swept Wing attached to a Cylindrical Fuselage

by

J. Weber and M. G. Joyce

Aerodynamics Dept., R.A.E., Farnborough

LONDON: HER MAJESTY'S STATIONERY OFFICE

1975

PRICE £2-20 NET

UDC 533.695.12 : 533.693.1 : 533.6.048.1 : 533.6.048.3 :
533.6.04 : 533.6.011.32

*CP No.1334
December 1973

INTERFERENCE PROBLEMS ON WING-FUSELAGE COMBINATIONS
PART IV THE DESIGN PROBLEM FOR A LIFTING SWEPT WING ATTACHED TO A CYLINDRICAL FUSELAGE

by

J. Weber
M. Gaynor Joyce

SUMMARY

The incompressible flow field past a circular cylindrical fuselage and a kinked infinite swept vortex, which lies in a plane through the axis of the fuselage, has been studied. In particular values for the downwash in this plane and on the surface of the fuselage have been determined numerically; the values are tabulated for four angles of sweep: 0, 30°, 45°, 60°.

The results are used to design wings of constant chord and infinite aspect ratio, attached to a cylindrical fuselage in midwing position, for which the chordwise load distribution is given and the spanwise distribution in the presence of the fuselage is required to be constant. It is shown how the interference effect varies with the angle of sweep, with the ratio R/c between the body radius and the wing chord, with the spanwise distance from the wing-body junction and with the thickness of the wing.

---

* Replaces RAE Technical Report 73190 - ARC 35294

CONTENTS

1 INTRODUCTION

In a previous report[1], we have considered the design of an unswept wing which, when attached to a cylindrical fuselage, produces a given chordwise load distribution which is constant across the span. In this Report, we extend the method to swept wings. We consider again an infinite cylindrical fuselage of circular cross section with the axis parallel to the main stream and a wing of constant chord and infinite span attached in the midwing position.

The present investigation is to be of an accuracy similar to that of linear wing-theory, which means we may assume that the bound vortices lie in a plane. We assume further that we may place the vortices in a plane through the axis of the fuselage, which means that we neglect the effect of the wing-body angle. This implies that we consider chordwise load distributions for which the required angle of twist is small near the wing-body junction. Each half of the nett wing can thus be represented by a chordwise distribution of semi-infinite swept vortices in a plane which crosses the fuselage at right angles.

The fuselage affects the flow near the wing-body junction in a way similar to that of an infinite reflection plate normal to the wing plane; thus the wing shape shows some similarity to that of an isolated wing, which produces the required loading, with its centre section at the wing-body junction. However there is a further effect caused by the finite curvature of the body. The aim of this Report is to examine this second effect; so we examine how the warp of the isolated wing has to be modified in order to retain the given load distribution.

As with the symmetrical wing-fuselage configuration considered in Ref.3, we choose inside the fuselage a vortex distribution which takes account of the reflection effect. This is done by taking a chordwise distribution of swept vortex lines of constant strength which are piecewise straight and have kinks at the wing-fuselage junctions and at the axis of the fuselage, as sketched in Fig.1.

We consider again, in section 2, first a single vortex in the presence of the fuselage and determine the strength of a source distribution on the surface of the fuselage such that the total normal velocity at the fuselage vanishes. From the known singularities in the wing plane and on the fuselage we determine the velocity component normal to the wing plane, v_z. We have computed values of v_z in the wing plane and on the fuselage. The difference between the values of v_z for the vortex in the presence of the fuselage and for the

isolated swept vortex, v_{zI}, is tabulated for four angles of sweep, $\phi = 0, 30^{o}, 45^{o}, 60^{o}$.

In section 3, we use the values of v_{zI} for a single vortex and determine by chordwise integration the downwash, which means in first-order theory the required wing warp, for a given chordwise load distribution. We select a few examples to demonstrate how the interference effect can vary with the angle of sweep, with the ratio R/c between the body radius and the wing chord, with the spanwise distance from the wing-body junction and with the type of chordwise load distribution. For the wing-body junction, we consider also the effect of the finite thickness of the wing on the additional wing warp caused by the presence of the fuselage.

2 A SINGLE KINKED SWEPT VORTEX IN THE PRESENCE OF A CIRCULAR CYLINDRICAL FUSELAGE

2.1 Velocities induced by the vortex

Let x, y, z be a cartesian system of coordinates and x, r, θ a system of cylindrical coordinates. We consider an infinitely long cylindrical fuselage of circular cross section $y^2 + z^2 = R^2 = 1$ and an infinite vortex in the plane $z = 0$ which is piecewise straight, swept by an angle $\pm\phi$ and which has kinks at $x = 0, y = R$, at $x = R \tan \phi$, $y = 0$ and at $x = 0, y = -R$. The position of the vortex is thus given by

$$x = |R - |y|| \tan \phi \quad . \tag{1}$$

The strength of the vortex is constant along the span and equal to Γ per unit length. In the following equations all lengths are made dimensionless by dividing by R.

For the velocity field induced by the vortex, expressions for the velocity components parallel to the x, y, z axes can be written down in analytic form. Using these one can obtain a formula for the velocity component normal to the surface of the fuselage, $v_{n\Gamma}(x,\theta)$; this formula is given in equation (A-2) of Appendix A. We learn from equation (A-2) that

$$\begin{aligned} v_{n\Gamma}(x,\theta) &= - v_{n\Gamma}(x,-\theta) \\ &= v_{n\Gamma}(x,\pi-\theta) \quad . \end{aligned} \tag{2}$$

2.2 Strength of the source distribution on the fuselage which makes the fuselage a stream surface

The strength $q(x,\theta)$ of the source distribution on the fuselage must satisfy the equation

$$v_{nq}(x,\theta) = - v_{n\Gamma}(x,\theta) \quad ,$$

where

$$v_{nq}(x,\theta) = \frac{q(x,\theta)}{2} + \int_{-\infty}^{\infty}\int_{0}^{2\pi} \frac{q(x',\theta')[1 - \cos(\theta - \theta')]\,d\theta'dx'}{4\pi\sqrt{(x - x')^2 + 2[1 - \cos(\theta - \theta')]}^3}$$

$$= \frac{q(x,\theta)}{2} + \int_{0}^{2\pi} \frac{q(x,\theta')}{4\pi}\,d\theta'$$

$$+ \int_{-\infty}^{\infty}\int_{0}^{2\pi} \frac{[q(x',\theta') - q(x,\theta')]\,[1 - \cos(\theta - \theta')]\,d\theta'dx'}{4\pi\sqrt{(x - x')^2 + 2[1 - \cos(\theta - \theta')]}^3} \quad . \qquad (3)$$

The source distribution $q(x,\theta)$ has the same planes of symmetry or anti-symmetry as $v_{n\Gamma}(x,\theta)$, so that

$$\int_{0}^{2\pi} q(x,\theta')d\theta' = 0 \quad . \qquad (4)$$

An approximate solution of equation (3) can be derived by an iterative procedure, such that the nth approximation $q^{(n)}(x,\theta)$ is derived from the $(n - 1)$th approximation by

$$q^{(n)}(x,\theta) = - 2v_{n\Gamma}(x,\theta)$$

$$- \int_{-\infty}^{\infty}\int_{0}^{2\pi} \frac{[q^{(n-1)}(x',\theta') - q^{(n-1)}(x,\theta')]\,[1 - \cos(\theta - \theta')]\,d\theta'dx'}{2\pi\sqrt{(x - x')^2 + 2[1 - \cos(\theta - \theta')]}^3} \quad ,$$

...(5)

where

$$q^{(0)}(x,\theta) = -2v_{n\Gamma}(x,\theta) \quad . \tag{6}$$

The first step in the iteration procedure leads to

$$q^{(1)}(x,\theta) = q^{(0)}(x,\theta) + \Delta^{(1)}q(x,\theta) \quad , \tag{7}$$

where

$$\Delta^{(1)}q(x,\theta) = -\int_{-\infty}^{\infty}\int_{0}^{2\pi} \frac{[q^{(0)}(x',\theta') - q^{(0)}(x,\theta')]\,[1 - \cos(\theta - \theta')]\,d\theta'dx'}{2\pi\sqrt{(x - x')^2 + 2[1 - \cos(\theta - \theta')]}^{3}} \quad . \tag{8}$$

We have computed values of $\Delta^{(1)}q(x,\theta)$ for $\theta = 15^{o}, 45^{o}, 90^{o}$; for $\phi = 30^{o}, 45^{o}, 60^{o}$. When $\Delta^{(1)}q(x,\theta)$ is approximated by the function

$$\Delta^{(1)}q(x,\theta) = A_1(x)\sin\theta + A_3(x)\sin 3\theta + A_5(x)\sin 5\theta \quad , \tag{9}$$

numerical values for $A_1(x)$, $A_3(x)$, $A_5(x)$ can be derived from the computed values $\Delta^{(1)}q(x,\theta = 15^{o})$, $\Delta^{(1)}q(x,\theta = 45^{o})$, $\Delta^{(1)}q(x,\theta = 90^{o})$. It was found that the maximum values of $|A_1(x;\phi)|$ are approximately the same for all values of ϕ . The ratio $|A_1(x;\phi)|_{max}\Big/|(q^{(0)}(x,\theta;\phi)|_{max}$ decreases from about 0.18 for $\phi = 0$ to about 0.11 for $\phi = 60^{o}$. The functions $|A_3(x)|$ and $|A_5(x)|$ have appreciably smaller values than $|A_1|_{max}$. The ratio $|A_3|_{max}/|A_1|_{max}$ is about 0.15 and $|A_5|_{max}/|A_1|_{max}$ is about 0.05, for all values of ϕ ; this means that $|A_3(x)|\Big/|q^{(0)}(x,\theta)|_{max} < 0.03$ and $|A_5(x)|\Big/|q^{(0)}(x,\theta)|_{max} < 0.01$. (These values suggest that, with computations for further values of ϕ , we need not compute $A_5(x)$; this would imply that it is sufficient to compute $\Delta^{(1)}q(x,\theta)$ for only two values of θ , say $\theta = 45^{o}$ and 90^{o}.) When we consider the magnitude of $|A_3(x)|\Big/|q^{(0)}(x,\theta)|_{max}$, we may conclude that it is sufficient to derive only an approximate value of

$$\Delta^{(2)}q(x,\theta) = -\int_{-\infty}^{\infty}\int_{0}^{2\pi} \frac{[\Delta q^{(1)}(x',\theta') - \Delta^{(1)}q(x,\theta')]\,[1 - \cos(\theta - \theta')]\,d\theta'dx'}{2\pi\sqrt{(x - x')^2 + 2[1 - \cos(\theta - \theta')]}^{3}} \quad \ldots(10)$$

by substituting for $\Delta q^{(1)}(x,\theta)$ the term $A_1(x) \sin\theta$. We therefore determine an approximate value of $\Delta^{(2)}q(x,\theta)$ in the form

$$\Delta^{(2)}q(x,\theta) = B(x) \sin\theta \quad , \tag{11}$$

with

$$B(x) = \Delta^{(2)}q(x,\theta = 90^{\circ}) = -\int_{-\infty}^{\infty}\int_{0}^{2\pi} \frac{[A_1(x') - A_1(x)] \sin\theta' \,(1 - \sin\theta')d\theta'dx'}{2\pi\sqrt{(x - x')^2 + 2(1 - \sin\theta')}^3} \quad . \tag{12}$$

The integral

$$I = \int_{0}^{2\pi} \frac{\sin\theta' \,(1 - \sin\theta')d\theta'}{\sqrt{(x - x')^2 + 2(1 - \sin\theta')}^3} = 2\int_{-\pi/2}^{\pi/2} \frac{\sin\theta' \,(1 - \sin\theta')d\theta'}{\sqrt{(x - x')^2 + 2(1 - \sin\theta')}^3}$$

can be expressed in terms of the complete elliptic integrals $\mathbf{K}(k)$, $\mathbf{E}(k)$ with

$$k^2 = \frac{4}{4 + (x - x')^2} \quad . \tag{13}$$

With the substitution $\theta' = 2\tau - \frac{\pi}{2}$, we obtain

$$I = \frac{-8}{\sqrt{(x - x')^2 + 4}} \int_{0}^{\pi/2} \frac{1 - 3\sin^2\tau + 2\sin^4\tau}{\sqrt{1 - k^2\sin^2\tau}^3} d\tau$$

$$= -\frac{\sqrt{(x - x')^2 + 4}}{2} \left\{(4 - k^2)\mathbf{E}(k) + (3k^2 - 4)\mathbf{K}(k)\right\} \quad . \tag{14}$$

Thus $B(x)$ can be determined from

$$B(x) = \int_{-\infty}^{\infty} \frac{\sqrt{(x - x')^2 + 4}}{4\pi} [A_1(x') - A_1(x)] [(4 - k^2)\mathbf{E} + (3k^2 - 4)\mathbf{K}] dx' \quad . (15)$$

We have computed values of $B(x)$; it was found that the maximum values of $|B(x;\phi)|$ are nearly independent of the value of ϕ and that the ratio $|B(x;\phi)|_{max} / |A_1(x;\phi)|_{max}$ is about 0.15 (a value similar to that for the ratio $|A_3(x;\phi)|_{max} / |A_1(x;\phi)|_{max}$. We conclude from this that we need not compute further modifications to the source distribution. This means that we consider the source distribution

$$q(x,\theta) = q^{(0)}(x,\theta) + \Delta^{(1)}q(x,\theta) + \Delta^{(2)}q(x,\theta) \quad , \qquad (16)$$

defined by equations (6), (9), (11), to be a sufficiently accurate solution of equation (3). We therefore derive in the following the velocity field induced by this source distribution which is given by the expression

$$q(x,\theta) = - 2v_{n\Gamma}(x,\theta) + [A_1(x) + B(x)] \sin\theta + A_3(x) \sin 3\theta + A_5(x) \sin 5\theta \quad . \qquad ...(17)$$

2.3 Downwash in the plane through the vortex and the axis of the fuselage

We consider now the velocity which the source distribution $q(x,\theta)$ on the fuselage induces in the plane $z = 0$, i.e. the plane through the vortex and the axis of the fuselage.

The velocity $v_{n\Gamma}(x,\theta)$ is an asymmetrical function of θ , $v_{n\Gamma}(x,\theta) = -v_{n\Gamma}(x,-\theta)$; as a consequence

$$q(x,\theta) = - q(x,-\theta) \quad .$$

Such a source distribution produces no velocity component tangential to the plane $\theta = 0$, i.e. $z = 0$. Therefore

$$v_{xq}(x,y,z = 0) = 0 \quad ,$$

$$v_{yq}(x,y,z = 0) = 0 \quad .$$

The source distribution $q(x,\theta)$ produces a velocity normal to the plane $z = 0$:

$$v_{zq}(x,y,0) = -\int_{-\infty}^{\infty}\int_{0}^{2\pi} \frac{q(x',\theta)}{4\pi} \frac{\sin\theta \, d\theta dx'}{\sqrt{(x - x')^2 + y^2 + 1 - 2y\cos\theta}^3} \quad . \tag{18}$$

For the numerical evaluation of v_{zq} , we have written equation (18) in the form

$$v_{zq}(x,y,0) = -\int_{-\infty}^{\infty}\int_{0}^{\pi} \frac{[q(x',\theta) - q(x,\theta)] \sin\theta \, d\theta dx'}{2\pi\sqrt{(x - x')^2 + y^2 + 1 - 2y\cos\theta}^3}$$

$$- \int_{0}^{\pi} \frac{q(x,\theta) \sin\theta \, d\theta}{\pi[y^2 + 1 - 2y\cos\theta]} \quad . \tag{19}$$

The evaluation of the integrals does not cause any difficulty, except for $y = 1$ and small values of $|x|$. It is shown in Appendix C that the function $v_{zq}(x,y = 1,0)$ behaves as

$$v_{zq}(x,y = 1,0) = -\frac{1}{8\pi} \frac{\sin\phi\cos\phi}{(1 + \cos\phi)^2} \log|x| + \frac{x}{|x|} I_5(\phi) + f(x;\phi) \quad , \tag{20}$$

where $I_5(\phi)$ can be evaluated numerically from single integrals and $f(x;\phi)$ is a finite continuous function.

It has been stated above that our aim is to determine the difference between the required shape of the wing when it is attached to the fuselage and the shape of the wing when it is attached to an infinite reflection plate. To obtain the corresponding interference term for the downwash of a single vortex, v_{zI} , we have to add to v_{zq} the difference between the downwash from the vortex with three kinks, $v_{z\wedge}$, and the downwash from the swept vortex (with one kink at $y = 1$), $v_{z\Lambda}$:

$$v_{zI}(x,y,0) = v_{zq}(x,y,0) + v_{z\wedge}(x,y,0) - v_{z\Lambda}(x,y,0) \quad . \tag{21}$$

A formula for $v_{z\wedge}(x,y,0) - v_{z\Lambda}(x,y,0)$ is given in equation (B-2) of Appendix B.

For $\phi = 45^o$ and $y = 1$, we have plotted values of v_{zq} and of v_{zI} in Fig.2. To provide a measure for the importance of the interference downwash, we have plotted also the term $0.2v_{z\Lambda}$. When we compare Fig.2 with the corresponding figure for a source line in the presence of a fuselage, Fig.5 of Ref.3 (where we have plotted v_{xq}, v_{xI} together with $-0.2v_{x\Lambda}$), we note that the interference effect seems to be more important with respect to the downwash from a vortex than with respect to the streamwise velocity component from a source line.

We have computed values of v_{zI} for the angles of sweep $\phi = 30^o$, 45^o, 60^o and for the spanwise stations $y/R = 1.0, 1.25, 2.0$. Values of v_{zI} are tabulated in Table 1. Fig.3 illustrates how the interference velocity, v_{zI} in the wing-body junction varies with the angle of sweep.

For $\phi = 45^o$, we have plotted, in Fig.4, v_{zI} for various spanwise stations as function of

$$\xi/R = x/R - (|y/R| - 1) \tan \phi \quad . \tag{22}$$

When we compare Fig.4 with the corresponding figure for a source line, Fig.7 of Ref.3, we note that $|v_{zI}|$ decreases more rapidly with increasing distance from the wing-body junction than the interference velocity $|v_{xI}|$ for a source line.

2.4 Downwash at points away from the plane $z = 0$

In practice, we are interested in designing wing-fuselage combinations with wings of finite thickness. We would therefore like to know how much the interference velocity at points away from the plane $z = 0$ differs from the interference velocity in the plane $z = 0$.

The velocity component v_{zq} induced by the source distribution $q(x,\theta)$ on the fuselage can be obtained from the relation

$$v_{zq}(x,y,z) = \int_{-\infty}^{\infty} \int_{0}^{2\pi} \frac{q(x',\theta')[z - \sin\theta']\, d\theta' dx'}{4\pi \sqrt{(x - x')^2 + (y - \cos\theta')^2 + (z - \sin\theta')^2}^3} \quad . \tag{23}$$

We are particularly interested in the downwash at the junction of a thick wing with the fuselage, i.e. at $y = \cos\theta$, $z = \sin\theta$. The values of v_{zq} at the fuselage can be derived from

$$v_{zq}(x,\theta) = \int_{-\infty}^{\infty}\int_{0}^{2\pi} \frac{q(x',\theta')[\sin\theta - \sin\theta']\,d\theta'dx'}{4\pi\sqrt{(x-x')^2 + 2[1-\cos(\theta-\theta')]}^3} + \sin\theta\,\frac{q(x,\theta)}{2} \quad . \tag{24}$$

This relation can be written in the form

$$v_{zq}(x,\theta) = \int_{-\infty}^{\infty}\int_{0}^{2\pi} \frac{[q(x',\theta') - q(x,\theta') - q(x',\theta) + q(x,\theta)][\sin\theta - \sin\theta']\,d\theta'dx'}{4\pi\sqrt{(x-x')^2 + 2[1-\cos(\theta-\theta')]}^3}$$

$$+ \int_{0}^{2\pi} \frac{[q(x,\theta') - q(x,\theta)][\sin\theta - \sin\theta']}{4\pi[1-\cos(\theta-\theta')]}\,d\theta' + \sin\theta\, q(x,\theta)$$

$$+ \sin\theta \int_{-\infty}^{\infty} \frac{q(x',\theta) - q(x,\theta)}{2\pi\sqrt{(x-x')^2+4}}\,[\mathbf{K}(k) - \mathbf{E}(k)]\,dx' \quad , \tag{25}$$

with

$$k^2 = \frac{4}{4 + (x-x')^2} \quad .$$

The numerical evaluation of $v_{zq}(x,\theta)$ from equation (25) does not cause any difficulty for $\theta \neq 0$. We have already determined the values for $\theta = 0$, since $v_{zq}(x,\theta = 0)$ from equation (25) is the same as $v_{zq}(x,y = 1,0)$ from equation (19).

For the wing-fuselage combination, the total velocity component v_z at the fuselage is given by the sum

$$v_z(x,\theta) = v_{zq}(x,\theta) + v_{z\wedge}(x,y = \cos\theta,\ z = \sin\theta) \quad . \tag{26}$$

Values of $v_{z\wedge}(x,y = \cos\theta, z = \sin\theta)$ can be derived from equation (A-1) of Appendix A.

Since our aim is to determine the difference between the velocity field induced by a planar vortex distribution in the presence of a fuselage and the

velocity field of the vortex distribution in the presence of a plane reflection plate, we define $v_{zI}(x,\theta)$ by

$$v_{zI}(x,\theta) = v_{zq}(x,\theta) + v_{z\wedge}(x,y = \cos\theta,\ z = \sin\theta) - v_{z\Lambda}(x,y = 1, z = \sin\theta) \quad . \qquad ...(27)$$

A relation for $v_{z\Lambda}$ can be derived from equation (B-1) of Appendix B.

Values of $v_{zI}(x,\theta)$ are quoted in Table 2. For $\phi = 0$ and $\phi = 45^{o}$, values of $v_{zI}(x,\theta)$ are plotted in Figs.5 and 6. The figures show that near $x = 0$ (where the vortex crosses the fuselage) the value of the interference downwash depends strongly on the value of θ. A somewhat different behaviour might be expected since a Taylor series expansion of v_{zI} with respect to z reads, except for $x = 0$, $y = R$,

$$\begin{aligned} v_{zI}(x,y,z) &= v_{zI}(x,y,0) + z\left(\frac{\partial v_{zI}(x,y,z)}{\partial z}\right)_{z=0} + \ldots . \\ &= v_{zI}(x,y,0) - z\left[\frac{\partial v_{xI}(x,y,0)}{\partial x} + \frac{\partial v_{yI}(x,y,0)}{\partial y}\right] + \ldots . \\ &= v_{zI}(x,y,0) + 0(z^{2}) \quad . \end{aligned} \qquad (28)$$

(We have not yet examined the behaviour of v_{xI} and v_{yI} when we approach the point $x = 0$, $y = R$, $z = 0$ along different paths.) Figs.5 and 6 show that the first two terms of the Taylor series do not give a reasonably accurate approximation to $v_{zI}(x,\theta)$ for $-1 + 0.5 \tan\phi < x/R < 1 + 0.5 \tan\phi$ and $\theta < 10^{o}$ say.

We note that Fig.5 replaces Fig.5 of Ref.1. The argument put forward on page 14 of Ref.1 for obtaining an estimate of the interference between a thick lifting wing and a fuselage is not sound. When we intend to represent a thick warped wing attached to the fuselage by singularity distributions in the plane of the wing and on the fuselage, we can retain source distributions on the part of the fuselage surface which is inside the thick wing. The downwash at the surface of the thick wing which is induced by a planar vortex distribution in the presence of the fuselage is related to the same source distribution $q(x,\theta)$ on the fuselage as is the downwash on the thin wing, but we have to evaluate the interference downwash at the surface of the thick wing.

2.5 Streamwise velocity at points away from the plane $z = 0$

We have noted above that the source distribution $q(x,\theta)$ on the fuselage does not produce a streamwise or a spanwise velocity in the plane $z = 0$; but at $z \neq 0$ finite velocities $v_{xq}(x,y,z \neq 0)$ and $v_{yq}(x,y,z \neq 0)$ are induced. The velocity component v_{xq} can be computed from the relation

$$v_{xq}(x,y,z) = \int_{-\infty}^{\infty} \int_{0}^{2\pi} \frac{q(x',\theta')(x - x')d\theta'dx'}{4\pi\sqrt{(x - x')^2 + (y - \cos\theta')^2 + (z - \sin\theta')^2}^3} \quad . \tag{29}$$

The interference velocity

$$v_{xI}(x,y,z) = v_{xq}(x,y,z) + v_{x\wedge}(x,y,z) - v_{x\Lambda}(x,y,z) \tag{30}$$

can be determined by deriving $v_{x\wedge}$ and $v_{x\Lambda}$ from equations (A-1) and (B-1). We have not yet computed any values of v_{xI} for $z \neq 0$. However, for an unswept vortex in the presence of a circular cylinder, Kramer[4] has computed (by an approximate method which differs from the present one) the pressure distribution at the fuselage and has tabulated values of the pressure coefficient, $C_p(x,\theta)$. Using Kramer's values of $C_p(x,\theta)$, one can derive values of $v_{xI}(x,\theta;\phi = 0)$:

$$v_{xI}(x,\theta;\phi = 0) = \frac{1}{4}\left[C_p(x,-\theta) - C_p(x,\theta)\right] - \frac{1}{2\pi}\frac{\sin\theta}{x^2 + \sin^2\theta} \quad . \tag{31}$$

Values of the ratio between the interference velocity $v_{xI}(x,\theta)$ and the streamwise velocity $v_{x\Gamma}(x,\theta)$ of the isolated vortex are plotted in Fig.7 (Kramer has given values of C_p for $|x| \geq 0.2$ only; therefore the values for $0 \leq x < 0.2$ are extrapolated.) Note that

$$\int_{0}^{\infty} v_{xI}(x,\theta;\phi = 0)dx = 0 \quad .$$

Values of the spanwise interference velocity at the fuselage can easily be found since

$$v_{yq}(x,\theta) + v_{y\wedge}(x,\theta) = - \tan\theta \, [v_{zq}(x,\theta) + v_{z\wedge}(x,\theta)] \quad .$$

We shall see in section 3.2 that when we intend to determine, to second-order accuracy, only the shape of a wing with finite thickness for which the vorticity distribution in the wing plane is given, then we do not require to know the values of the interference velocities $\Delta v_x(x,y,z)$, $\Delta v_y(x,y,z)$, which implies we do not need the values of $v_{xI}(x,y,z)$; $v_{yI}(x,y,z)$. However, if we want to know the pressure distribution at the fuselage and at the surface of the wing and in particular the difference, ΔC_p , between the pressure coefficients on the upper and lower surfaces of the wing, to second order, then a knowledge of $v_{xI}(x,y,z)$ (and for large angles of sweep perhaps also of $v_{yI}(x,y,z)$) would be required.

3 DESIGN OF THE MEAN SURFACE OF A WING-FUSELAGE COMBINATION FOR A GIVEN CHORDWISE LOAD DISTRIBUTION

3.1 Mean surface according to first-order theory

We consider now the design problem for a wing of constant chord, c , and infinite aspect ratio, attached to a circular fuselage in the midwing position.

We consider first the isolated wing which is to have a camber surface, $z_s^{(1)}(x,y)$, and a twist distribution, $\alpha^{(1)}(y)$, such that it produces a chordwise load distribution which is constant across the span:

$$\begin{aligned} - \Delta C_p(x,y) &= - \Delta C_p(\xi = x - (|y| - R) \tan\phi) \\ &= \ell(\xi) \quad . \end{aligned} \tag{32}$$

The superscript (1) denotes that the wing warp is to be obtained by first-order theory.

In first-order theory, such a load distribution can be represented by a chordwise distribution of infinite swept vortices in the chordal plane of strength $\gamma(\xi)$, where the vorticity is related to the pressure difference by the relation

$$\ell(\xi) = 2 \cos\phi \, \gamma(\xi) \quad . \tag{33}$$

Thus, the strength of an elemental strip of vortices, which are parallel to the leading edge, is

$$\gamma(\xi)dn = \gamma(\xi)\cos\phi\, d\xi = \tfrac{1}{2}\ell(\xi)d\xi \quad , \tag{34}$$

where dn is a length measured normal to the leading edge.

In first-order wing theory, one usually makes the assumption that the normal velocity at the wing surface can be approximated by the velocity component $v_z(x,y,0)$ in the chordal plane, so that the first-order boundary condition reads

$$\frac{\partial z_s^{(1)}(x,y)}{\partial x} - \alpha^{(1)}(y) = \frac{v_z(x,y,z=0)}{V_0} \quad , \tag{35}$$

where V_0 is the magnitude of the free stream velocity, which we take as unity.

For load distributions like those considered in this Report, where the direction of the vorticity vectors changes somewhere discontinuously, the downwash induced in the plane $z = 0$ tends logarithmically to infinity as we approach the station where the vorticity vectors have a kink. In a practical design, this difficulty can be avoided since one needs to determine the mean surface for a wing of finite thickness, $z_t(x,y)$; for this the first-order boundary condition can also be written in the form

$$\frac{\partial z_s^{(1)}(x,y)}{\partial x} - \alpha^{(1)}(y) = v_z(x,y,z_t(x,y)) \quad . \tag{36}$$

The design of the isolated wing (attached to an infinite reflection plate) can therefore be performed by means of equation (36).

We examine in the following only how the presence of the fuselage modifies the required shape of the mean surface. The interference downwash, $\Delta v_z(x,y,0)$, in the plane $z = 0$ is everywhere finite including the wing-body junction. We therefore consider first the interference downwash in the plane $z = 0$.

It follows from equation (34) that

$$\Delta v_z(x,y,0) = \frac{1}{2}\frac{c}{R}\int_0^1 \ell\left(\frac{x'}{c}\right)\frac{v_{zI}\left(\frac{x-x'}{R}, \frac{y}{R}, 0\right)}{\Gamma/R}\, d\left(\frac{x'}{c}\right) \quad , \tag{37}$$

where values of v_{zI} are given in Table 1.

It has been stated above, see equation (20), that, for $y = R$, v_{zq} and with it v_{zI} tend to infinity when $x' \to x$. For $y = R$, we therefore write equation (37) in the form

$$\Delta v_z(x,y = R,0) = \frac{1}{2}\frac{c}{R}\int_0^1 \left[\ell\left(\frac{x'}{c}\right) - \ell\left(\frac{x}{c}\right)\right] \frac{v_{zI}\left(\frac{x - x'}{R},1,0\right)}{\Gamma/R}\, d\left(\frac{x'}{c}\right)$$

$$+ \frac{1}{2}\frac{c}{R}\,\ell\left(\frac{x}{c}\right)\int_0^1 \frac{v_{zI}\left(\frac{x - x'}{R},1,0\right)}{\Gamma/R}\, d\left(\frac{x'}{c}\right) \quad . \tag{38}$$

For the second integral in equation (38) we use the relation

$$\int_0^1 \frac{v_{zI}\left(\frac{x - x'}{R},1,0\right)}{\Gamma/R}\, d\left(\frac{x'}{c}\right)$$

$$= -\frac{\sin\phi\cos\phi}{8\pi(1 + \cos\phi)^2}\left[\frac{x}{c}\log\frac{x}{c} + \left(1 - \frac{x}{c}\right)\log\left(1 - \frac{x}{c}\right) + \log\frac{c}{R} - 1\right]$$

$$+ I_5(\phi)\left(2\frac{x}{c} - 1\right) + \int_0^1 r_2\left(\frac{x - x'}{R}\,;\,\phi\right) d\left(\frac{x'}{c}\right) \quad , \tag{39}$$

where

$$r_2\left(\frac{x}{R}\,;\,\phi\right) = \frac{v_{zI}\left(\frac{x}{R},1,0\right)}{\Gamma/R} + \frac{\sin\phi\cos\phi}{8\pi(1 + \cos\phi)^2}\log\left|\frac{x}{R}\right| - \frac{x}{|x|}\,I_5(\phi) \tag{40}$$

is a finite continuous function, and values of $I_5(\phi)$ are given in Appendix C.

As an example, we have chosen the load distribution

$$\ell\left(\frac{\xi}{c}\right) = 4\alpha\cos\phi\sqrt{\frac{1 - \xi/c}{\xi/c}}\,, \quad 0 < \frac{\xi}{c} < 1 \tag{41}$$

which produces at spanwise stations far away from the fuselage, $|y| \gg R$, the downwash

$$v_z(\xi, y \gg R, 0) = -\alpha \quad .$$

Values of $\frac{\Delta v_z(x, y = R, 0)}{\alpha}$ for $\phi = 45^o$ and various values of c/R are plotted in Fig.8. Fig.8 shows that the interference downwash in the wing-body junction can be large and that it increases with increasing value of c/R , as is to be expected since Δv_z vanishes for $c/R \to 0$.

For $c/R = 5$ and various values of ϕ , values of $\Delta v_z(x, y = R, 0)$ are plotted in Fig.9. The figure shows that, for the flat-plate load distribution, the interference downwash does not depend much on the angle of sweep. The relatively weak dependence of Δv_z on the angle of sweep differs appreciably from the variation of the interference velocity $\Delta v_x(x, y = R, 0)$ for the displacement flow with the angle of sweep, shown in Figs.12, 14 and 15 of Ref.3.

We have computed values of $\Delta v_z(x, y = R, 0)$ also for the elliptic chordwise load distribution

$$\ell\left(\frac{\xi}{c}\right) = 16k \cos\phi \sqrt{\frac{\xi}{c}\left(1 - \frac{\xi}{c}\right)} \qquad (42)$$

which produces at spanwise stations far away from the fuselage the velocity

$$v_z(\xi, y \gg R, 0) = 2k\left(1 - 2\frac{\xi}{c}\right)$$

(the lift coefficient is $C_L = k2\pi \cos\phi$). Values of $\Delta v_z(x, y = R, 0)$ are plotted in Fig.10; they show a stronger dependence on the angle of sweep than the values of Δv_z related to the flat-plate load distribution. We can also expect that the variation of Δv_z with ϕ depends somewhat on the ratio c/R .

For $\phi = 45^o$, $c/R = 5$ and the flat-plate load distribution, the interference downwash has also been determined at spanwise stations away from the wing-body junction. In Fig.11, we have plotted Δv_z as a function of the coordinate ξ/c (where $x = (|y| - R) \tan\phi + \xi$) . We note that the magnitude of $|\Delta v_z|$ decreases rapidly with increasing y/R , as was to be expected from Fig.4.

When $\Delta v_z(x,y,0)$ is known, the required change of the wing surface can be derived from the first-order boundary condition, see equation (35)

$$\frac{\partial \Delta z^{(1)}(x,y)}{\partial x} = \frac{\partial \Delta z_s^{(1)}(x,y)}{\partial x} - \Delta\alpha^{(1)}(y)$$

$$= \Delta v_z(x,y,0) \quad . \tag{43}$$

If we keep the z-coordinate at the trailing edge, $z_{TE}(y) = z(\xi/c = 1,y)$, the same as for the isolated wing, then the additional wing warp $\Delta z^{(1)}$ is given by the relation

$$\frac{\Delta z^{(1)}(\xi,y)}{c} = -\int_{\xi/c}^{1} \Delta v_z\left(\frac{x}{c} = \left(\frac{|y|}{c} - \frac{R}{c}\right)\tan\phi + \frac{\xi'}{c}, y, 0\right) d\left(\frac{\xi'}{c}\right) \quad . \tag{44}$$

Values of $\Delta z^{(1)}$, derived from equation (44) and the downwash Δv_z given in Fig.11, are shown in Fig.12. The additional wing warp can be expressed as a change in the twist, $\Delta\alpha^{(1)}(y)$, and a change of the camber shape, $\Delta z_s^{(1)}$, where

$$\Delta\alpha^{(1)}(y) = -\int_{0}^{1} \Delta v_z(\xi',y,0) d\left(\frac{\xi'}{c}\right) \tag{45}$$

and

$$\frac{\Delta z_s^{(1)}(\xi,y)}{c} = \int_{0}^{\xi/c} \Delta v_z(\xi',y,0) d\left(\frac{\xi'}{c}\right) + \frac{\xi}{c}\Delta\alpha^{(1)}(y) \quad . \tag{46}$$

For an unswept wing, which, when attached to a fuselage, produces a flat-plate load distribution, the mean surface has the twist distribution $\Delta\alpha^{(1)}(y)$ and the camber $\Delta z_s^{(1)}(x,y)$. For a swept wing, the mean surface of the isolated wing is already twisted and cambered.

To illustrate the magnitude of the interference downwash for a combination of a swept wing and a fuselage, we have computed values of the downwash at the

centre section of the isolated wing, at a station far away from the centre section and at the wing-body junction. We have mentioned that, with a load distribution which is constant across the span, the downwash at the centre section must not be computed at $z = 0$. We have therefore computed the downwash for a constant finite value of z , namely $z/c = (R/c) \sin 10^{\circ}$ $= 0.2 \sin 10^{\circ} = 0.035$. To allow a proper comparison, we have computed also the interference downwash and the downwash of the sheared wing at $z \neq 0$. For $\phi = 45^{\circ}$ and the flat-plate load distribution, the various downwash distributions are shown in Fig.13 and for the elliptic chordwise load distribution of equation (42) in Fig.14. The figures show that, for a wing with 45° sweep, more of the difference between the required wing shape in the wing-body junction and the shape far away from the junction is produced by the reflection-plate effect than by the effect of the curvature of the body.

3.2 Mean surface according to second-order theory

When the effect of a fuselage on the streamwise velocity of a non-lifting wing-fuselage configuration is computed both by first-order and by second-order theory, it is found[2,3] that the inclusion of the various second-order terms can increase the computed interference effect appreciably. We would therefore like to learn something about the effect of second-order terms on the shape of a wing, with prescribed load distribution, when attached to a fuselage.

In this Report, we consider only configurations for which the axis of the fuselage is parallel to the main stream. Secondly, we consider only planar singularity distributions in a plane through the axis of the fuselage. A second-order wing theory is based on singularity distributions which lie in the chordal surface. This means that we can use the results of section 2 only for load distributions which produce a relatively small value for the twist $\alpha(y)$ near the centre section of the isolated wing ($\alpha(y)$ includes the angle of incidence for the sheared wing) and for the interference twist $\Delta\alpha(y)$; we thus ensure that the wing-body angle is sufficiently small for us to ignore its effect on the interference velocity $\underline{\Delta v}$. We consider therefore load distributions of low strength, i.e. with small lift coefficient C_L , and wings with finite thickness. We do not attempt to derive a complete second-order theory, but our aim is to determine the effect of the finite thickness on the additional wing warp caused by the presence of the fuselage. (We may note that, for a swept wing, the mean surface, derived from a load distribution which is constant across the span, may change its shape fairly rapidly near the centre section of the wing, so that the

terms $\partial z_s / \partial y$ and $d\alpha(y)/dy$ may be of first-order magnitude and be discontinuous at the centre section. When this is so, one could obtain a more accurate solution for the isolated wing, if one were to take account of the 'local dihedral effect', see for example Ref.5, and place the singularity distributions in semiplanes which are not coplanar. We cannot yet apply a similar procedure when we deal with a wing-fuselage combination. This is a further reason why we consider only load distributions of low strength.)

We consider wings of constant chord, with given thickness distribution $z_t(x,y)$ and given vorticity distribution $\ell(x,y)$ in the chordal plane $z = 0$. When designing the wings by second-order theory, one considers first a more accurate approximation to the condition that the total normal velocity at the wing surface must vanish than that given by equation (35). Secondly, one takes some account of the fact that the values of the various velocity components at the wing surface differ from those in the plane $z = 0$. The velocity components produced by the body interference vary also with the distance from the wing plane $z = 0$, so that we obtain a different modification to the wing shape, Δz_s, $\Delta\alpha(y)$ depending on whether we compute it by first-order or by second-order theory.

In a practical design case, one would also like to know how the second-order terms affect the pressure distribution on the surface of the wing. Such computations can be done for the isolated wing, see for example Ref.5; but, for wing-fuselage combinations with swept wings, we cannot consider the effect until we have computed values of $v_{xI}(x,y,z \neq 0)$.

Our next task is to derive an equation for the additional wing warp correct to second order, i.e. to the order $(C_L t/c)$, where t/c is the thickness-to-chord ratio. The boundary condition for the isolated wing can be written, to second-order accuracy[5], in the form

$$\left[\pm \frac{\partial z_t}{\partial x} + \frac{\partial z_s}{\partial x}\right]\left[1 + v_{xt}(x,y,0) \pm v_{x\ell}(x,y,0)\right]$$

$$+ \left[\pm \frac{\partial z_t}{\partial y} + \frac{\partial z_s}{\partial y}\right]\left[v_{yt}(x,y,0) \pm v_{y\ell}(x,y,0)\right]$$

$$= \pm v_{zt}(x,y,z_t \pm z_s) + v_{z\ell}(x,y,z_t \pm z_s) + \alpha(y) \quad . \qquad (47)$$

The velocity components with the suffix t are related to a source distribution in the wing plane and those with the suffix ℓ to the vorticity distribution $\ell(\xi)$. The upper and lower signs refer respectively to the upper and lower surfaces.

The boundary condition for the wing attached to the fuselage can be approximated by the relation:

$$\left[\pm\frac{\partial z_t}{\partial x}+\frac{\partial z_s}{\partial x}+\frac{\partial \Delta z_s}{\partial x}\right]\left[1+v_{xt}(x,y,0)+\Delta v_{xt}(x,y,0)\pm v_{x\ell}(x,y,0)\pm\Delta v_{x\ell}(x,y,0)\right]$$

$$+\left[\pm\frac{\partial z_t}{\partial y}+\frac{\partial z_s}{\partial y}+\frac{\partial \Delta z_s}{\partial y}\right]\left[v_{yt}(x,y,0)+\Delta v_{yt}(x,y,0)\pm v_{y\ell}(x,y,0)\pm\Delta v_{y\ell}(x,y,0)\right]$$

$$=\pm v_{zt}(x,y,z_t\pm z_s\pm\Delta z_s)\pm\Delta v_{zt}(x,y,z_t\pm z_s\pm\Delta z_s)$$

$$+v_{z\ell}(x,y,z_t\pm z_s\pm\Delta z_s)+\Delta v_{z\ell}(x,y,z_t\pm z_s\pm\Delta z_s)$$

$$+\alpha(y)+\Delta\alpha(y)\quad . \tag{48}$$

The term $\alpha(y)$ occurs in equation (47) since $z = 0$ represents the chordal surface of the wing and not a plane parallel to the mainstream. In equation (48), $z = 0$ represents again the chordal surface, which here differs both from that for the wing alone and from a plane which contains the body axis. However we assume that these differences can be ignored with respect to the perturbation velocities $\underline{v}$ and $\underline{\Delta v}$.

The terms Δv_{xt}, Δv_{yt}, Δv_{zt} are the components of the interference velocity for a wing-fuselage configuration with an uncambered wing at zero angle of incidence. The terms $\Delta v_{x\ell}$, $\Delta v_{y\ell}$, $\Delta v_{z\ell}$ are the components of the interference velocity which is so related to the load distribution $\ell(x,y)$ in the wing plane, that $\Delta v_{z\ell}$ denotes the same velocity component as Δv_z in section 3.1. We make use of the fact that the terms $\Delta v_{x\ell}(x,y,0)$ and $\Delta v_{y\ell}(x,y,0)$ vanish in the plane $z = 0$. Following the reasoning in section 3.2.1 of Ref.3, we neglect the terms Δv_{xt} and Δv_{yt} on the left-hand side of equation (48).

By subtracting equation (47) from equation (48), we obtain two relations for the interference terms, one referring to the upper surface of the wing, the

other referring to the lower surface. Adding these two equations, we obtain for Δz_s and $\Delta\alpha$ the relation

$$2\frac{\partial \Delta z_s}{\partial x}\left[1 + v_{xt}(x,y,0)\right] + 2\frac{\partial \Delta z_s}{\partial y} v_{yt}(x,y,0)$$

$$= v_{zt}(x,y,z_t + z_s + \Delta z_s) - v_{zt}(x,y,z_t + z_s)$$

$$- v_{zt}(x,y,z_t - z_s - \Delta z_s) + v_{zt}(x,y,z_t - z_s)$$

$$+ \Delta v_{zt}(x,y,z_t + z_s + \Delta z_s) - \Delta v_{zt}(x,y,z_t - z_s - \Delta z_s)$$

$$+ v_{z\ell}(x,y,z_t + z_s + \Delta z_s) - v_{z\ell}(x,y,z_t + z_s)$$

$$+ v_{z\ell}(x,y,z_t - z_s - \Delta z_s) - v_{z\ell}(x,y,z_t - z_s)$$

$$+ \Delta v_{z\ell}(x,y,z_t + z_s + \Delta z_s) + \Delta v_{z\ell}(x,y,z_t - z_s - \Delta z_s)$$

$$+ 2\Delta\alpha(y) \quad . \tag{49}$$

When we approximate $v_{zt}(x,y,z_t(x,y) + z^*)$ by the first two terms of a Taylor's series expansion with respect to z^*, then the sum

$$v_{zt}(x,y,z_t + z_s + \Delta z_s) - v_{zt}(x,y,z_t + z_s)$$

$$- v_{zt}(x,y,z_t - z_s - \Delta z_s) + v_{zt}(x,y,z_t - z_s)$$

can be replaced by

$$2\Delta z_s \left(\frac{\partial v_{zt}(x,y,z)}{\partial z}\right)_{z=z_t} \quad .$$

(We choose a Taylor series expansion from $z = z_t$, instead of from $z = 0$, because the derivative $\left(\partial v_{zt}/\partial z\right)_{z=0}$ at $z = 0$ tends to infinity at the centre section of the nett wing.) We approximate the derivative

$$(\partial v_{zt}(x,y,z)/\partial z)_{z=z_t}$$

by the terms

$$-\frac{\partial v_{xt}(x,y,z_t(x,y))}{\partial x} - \frac{\partial v_{yt}(x,y,z_t(x,y))}{\partial y} \quad .$$

It is known[3] that the values of Δv_{zt} are of similar magnitude to $0.1|v_{zt}|$; we therefore ignore the term

$$\Delta v_{zt}(x,y,z_t + z_s + \Delta z_s) - \Delta v_{zt}(x,y,z_t - z_s - \Delta z_s)$$

in equation (49). When we approximate $v_{z\ell}(x,y,z)$ by the first two terms of a Taylor series about $z = z_t$, then the term

$$v_{z\ell}(x,y,z_t + z_s + \Delta z_s) - v_{z\ell}(x,y,z_t + z_s)$$

$$+ v_{z\ell}(x,y,z_t - z_s - \Delta z_s) - v_{z\ell}(x,y,z_t - z_s)$$

can be neglected. Finally, we can replace the terms $v_{xt}(x,y,0)$, $v_{yt}(x,y,0)$ on the left-hand side of equation (49) by $v_{xt}(x,y,z_t)$, $v_{yt}(x,y,z_t)$. With these various modifications, equation (49) reads

$$\frac{\partial \Delta z_s}{\partial x} + \frac{\partial}{\partial x}(\Delta z_s v_{xt}(x,y,z_t)) + \frac{\partial}{\partial y}(\Delta z_s v_{yt}(x,y,z_t))$$

$$= \Delta\alpha(y) + \tfrac{1}{2}\left[\Delta v_{z\ell}(x,y,z_t + z_s + \Delta z_s) + \Delta v_{z\ell}(x,y,z_t - z_s - \Delta z_s)\right] \quad . \qquad (50)$$

We approximate this equation by the following:

$$\frac{\partial \Delta z^{(2)}(x,y)}{\partial x} = \frac{\partial \Delta z_s^{(2)}(x,y)}{\partial x} - \Delta\alpha^{(2)}(y)$$

$$= \Delta v_{z\ell}(x,y,z_t) - \frac{\partial}{\partial x}\left(\Delta z_s^{(1)} v_{xt}^{(1)}(x,y,z_t)\right) - \frac{\partial}{\partial y}\left(\Delta z_s^{(1)} v_{yt}^{(1)}(x,y,z_t)\right)$$

...(51)

where $\Delta z_s^{(1)}$ is the interference term derived by first-order theory and $v_{xt}^{(1)}$, $v_{yt}^{(1)}$ are the velocity components on the isolated wing, induced by the source distribution $q^{(1)}(x,y) = 2\frac{\partial z_t}{\partial x}$. We have added the superscript (2) in equation (51) to indicate that we expect $\Delta z_s^{(2)}$ and $\Delta\alpha^{(2)}$ to be accurate to second-order, in the sense that $\Delta z^{(2)}$ is correct to the order $(C_L t/c)$. We note that the term $\Delta z^{(2)}$ given by equation (51) varies linearly with the strength of the load distribution. If one were to take account of the wing-body angle, then one might expect that Δz would also contain a term of order C_L^2; one might further expect that this term would become more important for larger values of c/R.

When we compare equation (51) with the corresponding equation from first-order theory, equation (43), we note two differences; firstly the interference downwash $\Delta v_{z\ell}$ is computed at $z = z_t$ instead of at $z = 0$, secondly there is an additional term: $-\frac{\partial}{\partial x}(\Delta z_s v_{xt}) - \frac{\partial}{\partial y}(\Delta z_s v_{yt})$.

In section 2.4 we have computed values of v_{zI} at $z \neq 0$ only at the fuselage. We consider first how the interference downwash in the wing-body junction changes with the thickness of the wing, which means with the angle $\theta_J = \sin^{-1}\left(\frac{c}{R}\frac{z_t(x)}{c}\right)$. For $\phi = 45^\circ$, $c/R = 5$ and the flat-plate load distribution, the interference downwash $\Delta v_{z\ell}(x,\theta)$ is plotted in Fig.15 for various values of θ. (We note that, for a 10 per cent thick section and $c/R = 5$, the angle $\theta_J(x)$ has a maximum value $\theta_{J\,max} = 14.5^\circ$.) Fig.15 shows a strong dependence of $\Delta v_{z\ell}(x,\theta)$ on θ, even for relatively small values of θ. This behaviour seems to be at variance with the fact that a Taylor series expansion of $\Delta v_{z\ell}(x,y,z)$ in powers of z does not contain a linear term; the results shown in Fig.15 can however be explained by the variation of $v_{zI}(x,\theta)$ with increasing θ which is shown in Fig.6. When a thickness distribution is given, one can determine values of $\theta_J(x)$ and derive values of $\Delta v_{z\ell}(x,\theta_J(x))$ by interpolation between values similar to those shown in Fig.15. For the numerical examples we have chosen a 10 per cent thick RAE 101 section. For the flat-plate load distribution and $c/R = 5$, values of $\Delta v_{z\ell}(x,\theta_J)$ are plotted in Figs.16 and 17, for $\phi = 45^\circ$ and $\phi = 0$. The figures show also the values of $\Delta v_{z\ell}(x,\theta = 0)$. We see that the difference between $\Delta v_{z\ell}(x,\theta_J)$ and $\Delta v_{z\ell}(x,\theta = 0)$ is much larger for the swept wing than for the unswept wing. This is a consequence of the different variations of $v_{zI}(x,\theta;\phi)$ with θ for $\phi = 45^\circ$ and $\phi = 0$, shown in Figs.5 and 6. When the value of c/R is reduced, and the thickness distribution and the load distribution are kept constant, then

the difference between $\Delta v_{z\ell}(x,\theta_J)$ and $\Delta v_{z\ell}(x,\theta = 0)$ is also reduced because θ_J varies nearly linearly with c/R .

To determine the second and third terms on the right-hand side of equation (51), we use for $v_{xt}^{(1)}$ and $v_{yt}^{(1)}$ the approximate values given by the RAE Standard Method[6]. For a wing with constant chord and constant section shape across the span

$$v_{xt}^{(1)} \approx S^{(1)}(\xi) \cos \phi - K_2(y) f(\phi) \cos \phi \frac{dz_t}{d\xi} \tag{52}$$

$$v_{yt}^{(1)} \approx -(1 - |K_2(y)|) S^{(1)}(\xi) \sin \phi \tag{53}$$

(for details concerning the terms $S^{(1)}(\xi)$, $K_2(y)$, $f(\phi)$ see Ref.6). For the wing-body junction, where $K_2(y) = 1$ and $dK_2/dy = -8$, we obtain for $\Delta z_J^{(2)}$ the approximate equation:

$$\begin{aligned} \frac{d\Delta z_J^{(2)}}{dx} = {} & \Delta v_{z\ell}(x,\theta_J) \\ & - \frac{d\Delta z_{sJ}^{(1)}}{dx} \left[S^{(1)} \cos \phi - f(\phi) \cos \phi \frac{dz_t}{dx} \right] \\ & - \Delta z_{sJ}^{(1)} \left[\frac{dS^{(1)}}{dx} \cos \phi - f(\phi) \cos \phi \frac{d^2 z_t}{dx^2} - 8 S^{(1)}(x) \sin \phi \right] \end{aligned} \quad . \tag{54}$$

For the flat-plate load distribution and $c/R = 5$, we have plotted values of $d\Delta z_J^{(2)}/dx$ in Figs.16 and 17. (The small discontinuity in the curves at $x/c = 0.3$ is a consequence of the discontinuity in the slope $dS^{(1)}(x)/dx$ at $x/c = 0.3$.) For the swept wing, we note that the second-order results differ a great deal from the first-order results given by $d\Delta z_J^{(1)}/dx = \Delta v_{z\ell}(x,\theta = 0)$; the difference is less for the unswept wing. Fig.18 gives a comparison between the first- and second-order results for the elliptic chordwise loading.

For the swept wing and both types of chordwise load distribution, the change in twist produced by the body interference, $\Delta\alpha_J$, is less when we apply second-order theory than first-order theory; the maximum amount of camber is larger and the position of maximum camber is further rearwards. We have not derived the effect of the second-order terms on the wing shape away from the

junction, but we may assume that they are less important, because the fact that the linear term in the Taylor series expansion of $\Delta v_z(x,y,z)$ with respect to z vanishes is likely to have a more decisive influence on the difference between $\Delta v_z(x,y,z_t)$ and $\Delta v_z(x,y,z = 0)$ for $y > R$ than for $y = R$. As a consequence, we may expect that the change in the wing warp caused by the body interference varies less rapidly across the span when it is determined by second-order theory than by first-order theory.

In a practical design case, the thickness distribution and the pressure distribution on the upper surface of the wing attached to a fuselage at zero incidence may be prescribed. From this we can derive a first-order load distribution $\ell^{(1)}(x,y)$ by a procedure similar to that of equation (85) in Ref.5, when we substitute for $v_{xt}^{(1)}$ the sum $v_{xt}^{(1)} + \Delta v_{xt}^{(1)}$. The resulting load distribution varies most likely across the span, and the effect of the trailing vortices on the normal velocity at the surface of the fuselage has also to be considered. By applying the method developed in this Report, we can derive therefore only an estimate of the additional wing warp Δz, the accuracy of which would depend on the spanwise variation of the load distribution $\ell^{(1)}(x,y)$. When one neglects the interference velocities $\Delta v_{x\ell}$ and $\Delta v_{y\ell}$ at the surface of the wing, then one can improve the accuracy of the load distribution and of the mean surface of the isolated wing by a procedure similar to that suggested in section 3.2 of Ref.5. We can expect that $\Delta v_{x\ell}(x,y,z)$ contains a term of order (zC_L). We can also expect that the wing-body angle is not small, so that the application of the present method, which neglects the effect of the wing-body angle, can produce an error in Δz which may be of a magnitude similar to that of the second and third terms on the right-hand side of equation (51). In a practical application of the present method, we therefore suggest that these terms in equation (51) should be ignored, and that in the wing-body junction Δz_J should be derived from the interference downwash $\Delta v_{z\ell}(x,\theta_J)$ computed at θ_J,

$$\frac{d\Delta z_J}{dx} = \Delta v_{z\ell}(x,\theta_J) \tag{55}$$

and not from $\Delta v_{z\ell}(x,\theta = 0)$ computed at $\theta = 0$, i.e. not from equation (43). For spanwise stations away from the fuselage, one may expect that equation (43) produces a sufficiently accurate estimate of $\Delta z(x,y > R)$.

An examination of the accuracy of the proposed design procedure requires a method for determining the pressure distribution on a wing of given shape, when attached to a fuselage. The present work does not provide such a method. The results for a non-lifting wing fuselage configuration obtained by the panel method of A.M.O. Smith[7], see Fig.22 of Ref.3, cast doubts on the pressure distribution near the wing-body junction computed by any method which uses planar source panels of constant strength. We would prefer a computation which uses Roberts' program[8] (curved panels of varying source strength), but such a computation for a wing-body configuration, designed by the suggested procedure, has not yet been done. (We can expect that the geometry changes fairly rapidly near the wing-body junction, unless the body departs from a cylinder. This makes it necessary to use a large number of curved panels to describe the configuration.) So we do not yet know how useful the present method is for deriving a first estimate of $\Delta z^{(1)}$ in a practical design case. For this reason it does not seem important to extend the present work, for wings with infinite aspect ratio and constant spanwise load distribution, to the computation of the streamwise interference velocity at points away from the wing plane nor of the interference downwash at points away from the fuselage and the wing plane.

4 CONCLUSIONS

The present Report gives tabulated values of the difference between the downwash induced by a single kinked swept vortex in the presence of a circular cylindrical fuselage and the downwash induced by the vortex reflected at an infinite plate. These tables can be used to design wings of constant chord and infinite aspect ratio, attached in midwing position to a fuselage, such that the wing-fuselage combination produces a given chordwise load distribution which is constant across the span.

The method applies to fuselages for which the axis is parallel to the mainstream and to load distributions for which the resulting twist is small near the wing-body junction (the method neglects the effect of the wing-body angle). The computed interference effect on the wing warp is generally accurate only to first order, but it is shown how some account may be taken of the effect of the finite wing thickness on the additional wing warp.

It is found that the downwash caused by the body interference can be important, both for swept and unswept wings, since it can be of a magnitude comparable to that for the basic sheared wing.

In this Report, we have considered only configurations for which the axis of the fuselage is parallel to the mainstream. When the fuselage is set at an angle of incidence, α_B, to the mainstream and the load distribution over the wing remains unaltered, then (within first-order theory, in which the effect of a wing-body angle on the interference downwash can be neglected) the downwash in the wing plane would be altered only by the additional upwash from the flow past the isolated fuselage, $v_{zB} = \alpha_B(R/y)^2$. This implies that the twist would be reduced by $\alpha_B(R/y)^2$.

In a practical design case, the present method can give only an estimate of the additional wing warp since it does not take account of the spanwise variation of the load distribution. It seems therefore desirable to extend the method to general vorticity distributions in the plane $\theta = 0$.

For swept wings and load distributions which are constant across the span, one can obtain quite different values for the interference downwash in the wing-body junction depending on whether one computes the downwash in the wing plane or on the surface of the wing. It would be of interest to learn how the interference downwash varies with the distance from the wing plane for load distributions for an actual design, where it is likely that the bound vortices in the neighbourhood of the wing-body junction are less swept than the leading and trailing edges of the wing. For general load distributions, it may also be desirable to compute the streamwise interference velocity $\Delta v_{x\ell}$ at points away from the wing plane $(\Delta v_{x\ell}(x,y,z = 0) = 0)$ to learn whether $\Delta v_{x\ell}$ makes an important contribution to the pressure distribution on the wing.

When these extensions have been made, one might consider the more general configuration of a warped wing with finite thickness, attached to a fuselage of non-circular cross section in a low- or high-wing position, forming a non-zero angle with the body axis.

Appendix A

VELOCITY FIELD INDUCED BY A VORTEX WITH THREE KINKS

The velocity $\underset{\sim}{v}(x,y,z)$ induced by a vortex in $x' = |1 - |y'|| \tan\phi$, $z' = 0$ of constant strength Γ per unit length can be written in the form

$$
\begin{aligned}
\underset{\sim}{v}(x,y,z) = -\frac{\Gamma}{4\pi}\Bigg\{ & \frac{-z\underline{i} - z\tan\phi\,\underline{j} + [x + (y-1)\tan\phi]\underline{k}}{[x + (y-1)\tan\phi]^2 + z^2/\cos^2\phi} \times \\
& \times \left[\frac{1 - y + x\tan\phi}{\sqrt{x^2 + (y-1)^2 + z^2}} + \frac{y - \tan\phi\,(x - \tan\phi)}{\sqrt{(x - \tan\phi)^2 + y^2 + z^2}} \right] \\
& + \frac{-z\underline{i} + z\tan\phi\,\underline{j} + [x - (y+1)\tan\phi]\underline{k}}{[x - (y+1)\tan\phi]^2 + z^2/\cos^2\phi} \times \\
& \times \left[\frac{1 + y + x\tan\phi}{\sqrt{x^2 + (y+1)^2 + z^2}} - \frac{y + \tan\phi\,(x - \tan\phi)}{\sqrt{(x - \tan\phi)^2 + y^2 + z^2}} \right] \\
& + \frac{-z\underline{i} + z\tan\phi\,\underline{j} + [x - (y-1)\tan\phi]\underline{k}}{[x - (y-1)\tan\phi]^2 + z^2/\cos^2\phi} \times \\
& \times \left[\frac{1}{\cos\phi} - \frac{1 - y - x\tan\phi}{\sqrt{x^2 + (y-1)^2 + z^2}} \right] \\
& + \frac{-z\underline{i} - z\tan\phi\,\underline{j} + [x + (y+1)\tan\phi]\underline{k}}{[x + (y+1)\tan\phi]^2 + z^2/\cos^2\phi} \times \\
& \times \left[\frac{1}{\cos\phi} - \frac{1 + y - x\tan\phi}{\sqrt{x^2 + (y+1)^2 + z^2}} \right] \Bigg\}
\end{aligned}
\qquad \text{(A-1)}
$$

where $\underline{i}$, $\underline{j}$, $\underline{k}$ are unit vectors parallel to the x, y, z axes.

From this equation we obtain for the normal velocity $v_{n\Gamma}$ at the fuselage $y^2 + z^2 = 1$ the relation

$$v_{n\Gamma}(x,\theta) = -\frac{\Gamma}{4\pi}\left\{\frac{\sin\theta\,(x-\tan\phi)}{[x-(1-\cos\theta)\tan\phi]^2+\sin^2\theta/\cos^2\phi}\times\right.$$

$$\times\left[\frac{1-\cos\theta+x\tan\phi}{\sqrt{x^2+2(1-\cos\theta)}}+\frac{\cos\theta-\tan\phi\,(x-\tan\phi)}{\sqrt{(x-\tan\phi)^2+1}}\right]$$

$$+\frac{\sin\theta\,(x-\tan\phi)}{[x-(1+\cos\theta)\tan\phi]^2+\sin^2\theta/\cos^2\phi}\times$$

$$\times\left[\frac{1+\cos\theta+x\tan\phi}{\sqrt{x^2+2(1+\cos\theta)}}-\frac{\cos\theta+\tan\phi\,(x-\tan\phi)}{\sqrt{(x-\tan\phi)^2+1}}\right]$$

$$+\frac{\sin\theta\,(x+\tan\phi)}{[x+(1-\cos\theta)\tan\phi]^2+\sin^2\theta/\cos^2\phi}\times$$

$$\times\left[\frac{1}{\cos\phi}-\frac{1-\cos\theta-x\tan\phi}{\sqrt{x^2+2(1-\cos\theta)}}\right]$$

$$+\frac{\sin\theta\,(x+\tan\phi)}{[x+(1+\cos\theta)\tan\phi]^2+\sin^2\theta/\cos^2\phi}\times$$

$$\left.\times\left[\frac{1}{\cos\phi}-\frac{1+\cos\theta-x\tan\phi}{\sqrt{x^2+2(1+\cos\theta)}}\right]\right\}. \qquad \text{(A-2)}$$

For $x = 0$

$$v_{n\Gamma}(x=0,\theta) = +\frac{\Gamma}{4\pi}\sin\phi\cos\phi\left[\frac{\sqrt{1+\cos\theta}}{\sqrt{2}+\cos\phi\sqrt{1-\cos\theta}}+\frac{\sqrt{1-\cos\theta}}{\sqrt{2}+\cos\phi\sqrt{1+\cos\theta}}\right]. \qquad \text{...(A-3)}$$

For small values of $|x|$ and small values of $|\theta|$, the leading terms in the relation for $v_{n\Gamma}$ are

$$v_{n\Gamma} = -\frac{\Gamma}{4\pi}\left\{\frac{2x\theta\cos^3\phi\,(x^2+\theta^2)}{[x^2\cos^2\phi+\theta^2]^2} + \frac{\theta\sin\phi\cos\phi\,[2x^4\cos^2\phi + x^2\theta^2\cos^2\phi - \theta^4]}{\sqrt{x^2+\theta^2}\,[x^2\cos^2\phi+\theta^2]^2} + \ldots.\right\} . \quad (A\text{-}4)$$

We may note here that, if the swept vortex outside the fuselage were continued inside the fuselage without a kink at the body junction then, for small values of $|x|$ and small values of $|\theta|$, the normal velocity would behave like

$$-\frac{\Gamma}{2\pi}\frac{\theta\sin\phi + \ldots}{x^2\cos^2\phi + \theta^2 + \ldots} .$$

This type of singular behaviour is of course due to the fact that we are considering an isolated vortex.

Appendix B

VELOCITY FIELD INDUCED BY A SWEPT VORTEX

The velocity $\underline{v}_{\Lambda}(x,y,z)$ induced by a vortex in $x' = |y' - 1| \tan\phi$, $z' = 0$ (i.e. a vortex with a kink at $x' = 0$, $y' = 1$) of constant strength Γ per unit length can be written in the form

$$\underline{v}_{\Lambda}(x,y,z) = -\frac{\Gamma}{4\pi}\left\{\frac{-z\underline{i} - z\tan\phi\,\underline{j} + [x + (y-1)\tan\phi]\underline{k}}{[x + (y-1)\tan\phi]^2 + z^2/\cos^2\phi} \times \right.$$

$$\times\left[\frac{1 - y + x\tan\phi}{\sqrt{x^2 + (y-1)^2 + z^2}} + \frac{1}{\cos\phi}\right]$$

$$+\frac{-z\underline{i} + z\tan\phi\,\underline{j} + [x - (y-1)\tan\phi]\underline{k}}{[x - (y-1)\tan\phi]^2 + z^2/\cos^2\phi} \times$$

$$\left.\times\left[\frac{1}{\cos\phi} - \frac{1 - y - x\tan\phi}{\sqrt{x^2 + (y-1)^2 + z^2}}\right]\right\} \quad . \qquad \text{(B-1)}$$

When we combine equations (A-1) and (B-1) then we obtain for the z-component of the velocity $\underline{v}_{\wedge} - \underline{v}_{\Lambda}$ in the plane $z = 0$:

$$v_{z\wedge}(x,y,0) - v_{z\Lambda}(x,y,0)$$

$$= -\frac{\Gamma}{4\pi}\left\{\frac{1}{x + (y-1)\tan\phi}\left[\frac{y - \tan\phi\,(x - \tan\phi)}{\sqrt{(x - \tan\phi)^2 + y^2}} - \frac{1}{\cos\phi}\right]\right.$$

$$+\frac{1}{x - (y+1)\tan\phi}\left[\frac{1 + y + x\tan\phi}{\sqrt{x^2 + (y+1)^2}} - \frac{y + \tan\phi\,(x - \tan\phi)}{\sqrt{(x - \tan\phi)^2 + y^2}}\right]$$

$$\left.+\frac{1}{x + (y+1)\tan\phi}\left[\frac{1}{\cos\phi} - \frac{1 + y - x\tan\phi}{\sqrt{x^2 + (y+1)^2}}\right]\right\} \quad . \qquad \text{(B-2)}$$

Appendix C

THE BEHAVIOUR OF $v_{zq}(x,y = 1,0)$ FOR SMALL VALUES OF $|x|$

The function $v_{zq}(x,y = 1,0)$, i.e. in the body junction, is singular when x tends to zero. The singular behaviour arises from the integral

$$\int_{-d}^{d} dx' \int_{0}^{\delta} \frac{v_{n\Gamma}(x',\theta)\theta d\theta}{\pi\sqrt{(x - x')^2 + \theta^2}^3}$$

and the two leading terms in the relation for $v_{n\Gamma}$, given by equation (A-4).

By a technique similar to the one used in Appendix B of Ref.3, it can be shown that the second term in the relation for $v_{n\Gamma}$, equation (A-4), produces for $v_{zq}(x,1,0)$ a behaviour like $\kappa \log |x|$ with

$$\kappa = -\frac{1}{8\pi} \frac{\sin\phi \cos\phi}{(1 + \cos\phi)^2} \quad .$$

The first term in the relation for $v_{n\Gamma}$ given by equation (A-4) produces a discontinuity, $\frac{x}{|x|} I_5(\phi)$, in the values of $v_{zq}(x,1,0)$ as x tends to zero. I_5 is given by the relation

$$I_5 = \lim_{x \to +0} \left(-\frac{\cos^3\phi}{2\pi^2} \int_{-d}^{d} \int_{0}^{\delta} \left\{ \frac{x'(x'^2 + \theta^2)}{\left[x'^2 \cos^2\phi + \theta^2\right]^2} - \frac{x(x^2 + \theta^2)}{\left[x^2 \cos^2\phi + \theta^2\right]^2} \right\} \times \right.$$

$$\times \frac{\theta^2 d\theta dx'}{\sqrt{(x - x')^2 + \theta^2}^3}$$

$$\left. - \frac{\cos^3\phi}{\pi^2} \int_{0}^{\delta} \frac{x(x^2 + \theta^2)d\theta}{\left[x^2 \cos^2\phi + \theta^2\right]^2} \right) \quad .$$

The single integral has the value $-\frac{1 + \cos^2\phi}{4\pi}$. By a procedure similar to that in Appendix B of Ref.2, the double integral can be expressed as a single integral:

$$I_5 = -\frac{1+\cos^2\phi}{4\pi}$$

$$-\frac{\cos^3\phi}{2\pi^2}\int_{-\infty}^{\infty}\left\{\frac{1}{\tau}+\frac{(1+\tau)^3[\tau^2(2\cos^2\phi-3\sin^2\phi)-2(1+\tau)^2\cos^4\phi]}{2\tau^2[\tau^2-(1+\tau)^2\cos^2\phi]^2}\right.$$

$$-\frac{|1+\tau|(1+\tau)[\tau^2(2\cos^2\phi-\sin^2\phi)-2(1+\tau)^2\cos^2\phi]}{2\cos\phi\sqrt{|\tau^2-(1+\tau)^2\cos^2\phi|^5}}f_1(\tau)$$

$$-\frac{\tau^2(2\cos^2\phi-3\sin^2\phi)-2\cos^4\phi}{2\tau^2[\tau^2-\cos^2\phi]^2}$$

$$\left.+\frac{\tau^2(2\cos^2\phi-\sin^2\phi)-2\cos^2\phi}{2\cos\phi\sqrt{|\tau^2-\cos^2\phi|^5}}f_2(\tau)\right\}d\tau$$

where $f_1(\tau) = \tan^{-1}\dfrac{\sqrt{\tau^2-(1+\tau)^2\cos^2\phi}}{|1+\tau|\cos\phi}$ for

$$-\infty < \tau < -\frac{\cos\phi}{1+\cos\phi} \quad \text{and} \quad \frac{\cos\phi}{1-\cos\phi} < \tau < \infty$$

and $f_1(\tau) = \frac{1}{2}\log\dfrac{(1+\tau)\cos\phi+\sqrt{(1+\tau)^2\cos^2\phi-\tau^2}}{(1+\tau)\cos\phi-\sqrt{(1+\tau)^2\cos^2\phi-\tau^2}}$ for

$$-\frac{\cos\phi}{1+\cos\phi} < \tau < \frac{\cos\phi}{1-\cos\phi}$$

and $f_2(\tau) = \tan^{-1}\dfrac{\sqrt{\tau^2-\cos^2\phi}}{\cos\phi}$ for

$$-\infty < \tau < -\cos\phi \quad \text{and} \quad \cos\phi < \tau < \infty$$

and $f_2(\tau) = \frac{1}{2}\log\dfrac{\cos\phi+\sqrt{\cos^2\phi-\tau^2}}{\cos\phi-\sqrt{\cos^2\phi-\tau^2}}$ for

$$-\cos\phi < \tau < \cos\phi \quad .$$

We have evaluated the integral numerically and have obtained the values

ϕ	I_5
0	-0.10610
30^o	-0.10283
45^o	-0.09906
60^o	-0.09337

The remaining contributions to $v_{zq}(x,1,0)$ are finite continuous functions. Thus $v_{zq}(x,1,0)$ behaves as

$$v_{zq}(x,y = 1,0) = -\frac{1}{8\pi}\frac{\sin\phi\cos\phi}{(1+\cos\phi)^2}\log|x| + \frac{x}{|x|}I_5(\phi) + f(x;\phi) \qquad \text{(C-1)}$$

where $f(x;\phi)$ is a finite continuous function.

Table 1

DOWNWASH COMPONENT OF THE INTERFERENCE VELOCITY ON THE WING, $\frac{v_{zI}(x,y,z=0)}{\Gamma/R}$, FOR A SINGLE VORTEX

y/R / x/R	$\phi = 0$			$\phi = 30^\circ$			$\phi = 45^\circ$			$\phi = 60^\circ$		
	1.0	1.25	2.0	1.0	1.25	2.0	1.0	1.25	2.0	1.0	1.25	2.0
-20.0	0.0080	0.0051	0.0020	0.0048	0.0032	0.0013	0.0036	0.0024	0.0011	0.0024	0.0016	0.0007
-10.0	0.0161	0.0104	0.0041	0.0102	0.0067	0.0029	0.0077	0.0052	0.0024	0.0054	0.0038	0.0018
-8.0	0.0201	0.0129	0.0051	0.0129	0.0085	0.0037	0.0098	0.0066	0.0030	0.0068	0.0048	0.0023
-6.0	0.0266	0.0170	0.0066	0.0174	0.0114	0.0050	0.0134	0.0090	0.0041	0.0095	0.0066	0.0031
-5.0	0.0314	0.0200	0.0075	0.0208	0.0137	0.0058	0.0162	0.0108	0.0049	0.0116	0.0079	0.0038
-4.5	0.0343	0.0217	0.0081	0.0230	0.0151	0.0064	0.0179	0.0120	0.0053	0.0129	0.0086	0.0042
-4.0	0.0378	0.0238	0.0087	0.0256	0.0168	0.0070	0.0200	0.0134	0.0059	0.0145	0.0099	0.0047
-3.5	0.0418	0.0260	0.0093	0.0287	0.0188	0.0076	0.0226	0.0150	0.0065	0.0164	0.0110	0.0052
-3.0	0.0466	0.0288	0.0098	0.0324	0.0210	0.0083	0.0257	0.0169	0.0072	0.0188	0.0127	0.0058
-2.5	0.0522	0.0316	0.0102	0.0369	0.0236	0.0090	0.0295	0.0193	0.0080	0.0217	0.0146	0.0065
-2.0	0.0589	0.0347	0.0104	0.0425	0.0267	0.0096	0.0343	0.0220	0.0087	0.0254	0.0168	0.0073
-1.75	0.0628	0.0361	0.0102	0.0459	0.0284	0.0098	0.0372	0.0236	0.0090	0.0277	0.0181	0.0076
-1.5	0.0670	0.0374	0.0099	0.0496	0.0300	0.0099	0.0404	0.0252	0.0092	0.0303	0.0196	0.0080
-1.25	0.0717	0.0383	0.0093	0.0537	0.0315	0.0098	0.0441	0.0268	0.0093	0.0332	0.0211	0.0083
-1.0	0.0768	0.0384	0.0083	0.0584	0.0326	0.0094	0.0483	0.0283	0.0093	0.0368	0.0228	0.0084
-0.9	0.0790	0.0381	0.0078	0.0605	0.0330	0.0092	0.0502	0.0288	0.0091	0.0383	0.0233	0.0084
-0.8	0.0812	0.0375	0.0072	0.0626	0.0332	0.0089	0.0522	0.0292	0.0090	0.0401	0.0238	0.0085
-0.7	0.0836	0.0365	0.0065	0.0649	0.0332	0.0086	0.0544	0.0295	0.0089	0.0420	0.0243	0.0084
-0.6	0.0861	0.0350	0.0058	0.0674	0.0328	0.0081	0.0567	0.0296	0.0085	0.0439	0.0247	0.0083
-0.5	0.0886	0.0328	0.0050	0.0701	0.0320	0.0076	0.0594	0.0294	0.0082	0.0462	0.0251	0.0082
-0.4	0.0914	0.0295	0.0041	0.0731	0.0306	0.0070	0.0623	0.0287	0.0077	0.0489	0.0248	0.0080
-0.3	0.0944	0.0249	0.0031	0.0767	0.0282	0.0063	0.0658	0.0268	0.0073	0.0520	0.0244	0.0078
-0.2	0.0979	0.0186	0.0021	0.0812	0.0242	0.0055	0.0704	0.0249	0.0068	0.0561	0.0232	0.0075
-0.1	0.1018	0.0101	0.0011	0.0875	0.0181	0.0047	0.0772	0.0206	0.0062	0.0628	0.0211	0.0071
-0.05	0.1039	0.0052	0.0005	0.0926	0.0141	0.0042	0.0831	0.0178	0.0058	0.0689	0.0196	0.0069
-0.02	0.1052	0.0021	0.0002	0.0982	0.0114	0.0040	0.0902	0.0158	0.0055	0.0765	0.0185	0.0068
0	±0.1061	0.0	0.0	-	0.0094	0.0038	-	0.0143	0.0054	-	0.0177	0.0067
0.02	-0.1052	-0.0021	-0.0002	-0.1059	0.0085	0.0036	-0.1068	0.0129	0.0053	-0.1094	0.0165	0.0066
0.05	-0.1039	-0.0052	-0.0005	-0.1097	0.0053	0.0033	-0.1121	0.0105	0.0051	-0.1157	0.0146	0.0064
0.1	-0.1018	-0.0101	-0.0011	-0.1111	0.0006	0.0028	-0.1154	0.0064	0.0047	-0.1202	0.0116	0.0062
0.2	-0.0979	-0.0186	-0.0021	-0.1107	-0.0086	0.0018	-0.1167	-0.0021	0.0039	-0.1232	0.0052	0.0056
0.3	-0.0944	-0.0249	-0.0031	-0.1090	-0.0166	0.0008	-0.1161	-0.0100	0.0031	-0.1238	-0.0017	0.0050
0.4	-0.0914	-0.0295	-0.0041	-0.1071	-0.0229	-0.0002	-0.1151	-0.0166	0.0023	-0.1237	-0.0077	0.0044
0.5	-0.0886	-0.0328	-0.0050	-0.1053	-0.0279	-0.0011	-0.1138	-0.0223	0.0014	-0.1230	-0.0134	0.0037
0.6	-0.0861	-0.0350	-0.0058	-0.1034	-0.0317	-0.0021	-0.1125	-0.0268	0.0005	-0.1221	-0.0183	0.0031
0.7	-0.0836	-0.0365	-0.0065	-0.1014	-0.0347	-0.0030	-0.1110	-0.0308	-0.0002	-0.1210	-0.0226	0.0024
0.8	-0.0812	-0.0375	-0.0072	-0.0995	-0.0370	-0.0038	-0.1094	-0.0337	-0.0012	-0.1200	-0.0262	0.0017
0.9	-0.0790	-0.0381	-0.0078	-0.0976	-0.0388	-0.0046	-0.1078	-0.0362	-0.0020	-0.1190	-0.0296	0.0009
1.0	-0.0768	-0.0384	-0.0083	-0.0957	-0.0401	-0.0053	-0.1062	-0.0382	-0.0028	-0.1179	-0.0321	0.0003
1.25	-0.0717	-0.0383	-0.0093	-0.0910	-0.0420	-0.0068	-0.1020	-0.0413	-0.0044	-0.1149	-0.0370	-0.0014
1.5	-0.0670	-0.0374	-0.0099	-0.0864	-0.0426	-0.0080	-0.0980	-0.0434	-0.0059	-0.1117	-0.0408	-0.0027
1.75	-0.0628	-0.0361	-0.0102	-0.0825	-0.0424	-0.0088	-0.0940	-0.0441	-0.0069	-0.1084	-0.0432	-0.0039
2.0	-0.0589	-0.0347	-0.0104	-0.0782	-0.0417	-0.0095	-0.0901	-0.0442	-0.0079	-0.1050	-0.0444	-0.0050
2.5	-0.0522	-0.0316	-0.0102	-0.0708	-0.0396	-0.0101	-0.0828	-0.0432	-0.0091	-0.0985	-0.0455	-0.0066
3.0	-0.0466	-0.0288	-0.0098	-0.0646	-0.0371	-0.0103	-0.0763	-0.0414	-0.0096	-0.0923	-0.0451	-0.0077
3.5	-0.0418	-0.0260	-0.0093	-0.0587	-0.0345	-0.0101	-0.0705	-0.0392	-0.0098	-0.0867	-0.0440	-0.0084
4.0	-0.0378	-0.0238	-0.0087	-0.0540	-0.0322	-0.0098	-0.0654	-0.0372	-0.0098	-0.0816	-0.0428	-0.0088
4.5	-0.0343	-0.0217	-0.0081	-0.0497	-0.0300	-0.0094	-0.0609	-0.0352	-0.0097	-0.0769	-0.0412	-0.0091
5.0	-0.0314	-0.0200	-0.0075	-0.0460	-0.0280	-0.0090	-0.0568	-0.0332	-0.0095	-0.0726	-0.0397	-0.0092
6.0	-0.0266	-0.0170	-0.0066	-0.0397	-0.0245	-0.0082	-0.0499	-0.0297	-0.0089	-0.0651	-0.0366	-0.0091
8.0	-0.0201	-0.0129	-0.0051	-0.0311	-0.0194	-0.0067	-0.0397	-0.0241	-0.0077	-0.0535	-0.0310	-0.0086
10.0	-0.0161	-0.0104	-0.0041	-0.0253	-0.0158	-0.0057	-0.0328	-0.0201	-0.0067	-0.0452	-0.0267	-0.0078
20.0	-0.0080	-0.0051	-0.0020	-0.0131	-0.0083	-0.0031	-0.0176	-0.0110	-0.0039	-0.0255	-0.0156	-0.0051

Table 2

DOWNWASH COMPONENT OF THE INTERFERENCE VELOCITY ON THE FUSELAGE, $\frac{v_{zI}(x,\theta)}{\Gamma/R}$, FOR A SINGLE VORTEX

θ / x/R	φ = 0				φ = 30°				φ = 45°				φ = 60°			
	0	5°	10°	15°	0	5°	10°	15°	0	5°	10°	15°	0	5°	10°	15°
-20	0.0080	0.0079	0.0075	0.0069	0.0048	0.0048	0.0046	0.0042	0.0036	0.0035	0.0034	0 0031	0.0024	0.0024	0.0023	0.0021
-10	0.0161	0.0158	0.0151	0.0140	0.0102	0.0100	0.0096	0.0089	0.0077	0 0076	0.0072	0.0067	0.0054	0 0053	0.0051	0.0047
-8	0.0201	0.0198	0.0189	0.0174	0.0129	0.0127	0.0122	0.0113	0.0098	0.0097	0.0093	0.0086	0.0068	0.0068	0.0065	0.0060
-6	0.0266	0.0262	0.0250	0.0230	0.0174	0.0172	0 0164	0.0152	0.0134	0.0132	0.0127	0.0118	0.0095	0.0094	0.0090	0.0084
-5	0.0314	0.0309	0.0294	0.0271	0.0208	0.0205	0.0196	0.0182	0.0162	0.0160	0.0153	0.0142	0.0116	0.0114	0.0110	0.0102
-4.5	0.0343	0.0338	0.0322	0.0295	0.0230	0.0227	0.0217	0.0201	0.0179	0.0177	0.0170	0.0158	0.0129	0.0127	0.0122	0 0114
-4	0.0378	0.0372	0.0354	0.0324	0.0256	0.0252	0.0241	0.0223	0.0200	0.0198	0.0189	0.0176	0.0145	0.0143	0.0137	0.0128
-3.5	0.0418	0.0411	0.0391	0.0357	0.0287	0.0282	0.0270	0.0250	0.0226	0.0222	0.0213	0.0198	0.0164	0.0162	0.0155	0.0145
-3	0.0466	0.0458	0.0434	0.0395	0.0324	0.0319	0.0304	0.0281	0.0257	0.0253	0.0242	0.0225	0.0188	0.0185	0.0178	0.0166
-2 5	0.0522	0.0512	0.0484	0 0438	0.0369	0.0364	0.0346	0.0319	0.0295	0.0291	0.0278	0.0257	0.0217	0 0214	0.0205	0.0191
-2	0.0589	0.0577	0.0542	0.0485	0.0425	0.0418	0.0397	0.0363	0.0343	0.0338	0 0322	0.0296	0.0254	0.0251	0.0240	0 0222
-1.75	0.0628	0.0614	0.0574	0.0509	0.0459	0.0450	0.0426	0.0388	0.0372	0.0361	0.0348	0.0319	0.0277	0 0273	0.0261	0 0241
-1.5	0.0670	0.0654	0.0606	0.0530	0.0496	0.0486	0.0458	0.0413	0.0404	0.0397	0 0376	0.0343	0.0303	0 0298	0 0284	0 0261
-1.25	0.0717	0.0696	0.0637	0 0545	0.0537	0.0526	0.0492	0.0438	0.0441	0.0432	0.0407	0.0368	0.0332	0 0327	0.0310	0 0283
-1	0.0768	0.0741	0 0663	0.0545	0.0584	0 0569	0.0525	0 0458	0.0483	0.0472	0.0441	0.0392	0 0368	0.0361	0.0340	0.0307
-0.9	0.0790	0.0758	0 0670	0 0537	0.0605	0.0588	0.0539	0.0463	0.0502	0.0490	0 0454	0.0400	0.0383	0.0375	0.0352	0.0315
-0.8	0.0812	0.0776	0.0673	0.0522	0.0626	0.0606	0.0550	0.0465	0.0522	0.0508	0.0468	0.0406	0.0401	0.0392	0.0365	0.0323
-0.7	0.0836	0.0792	0.0670	0 0496	0.0649	0.0626	0.0560	0.0463	0.0544	0.0527	0.0480	0.0410	0.0420	0.0408	0 0375	0.0330
-0.6	0.0861	0.0805	0.0656	0.0453	0.0674	0.0646	0.0567	0.0453	0.0567	0.0547	0.0491	0.0408	0 0439	0.0426	0.0389	0.0334
-0.5	0.0886	0.0813	0.0625	0 0385	0.0701	0.0664	0.0565	0.0429	0.0594	0.0568	0 0497	0 0400	0.0462	0.0446	0.0400	0.0335
-0.4	0 0914	0.0811	0 0563	0.0283	0.0731	0.0681	0.0550	0.0387	0.0623	0.0588	0.0496	0.0378	0.0489	0.0465	0.0405	0.0327
-0.3	0.0944	0.0783	0.0446	0 0136	0 0767	0.0688	0.0507	0.0315	0.0658	0.0604	0.0476	0.0336	0.0520	0.0485	0 0402	0.0309
-0.2	0.0979	0.0682	0.0235	-0.0036	0 0812	0.0665	0.0408	0.0212	0.0704	0.0603	0.0420	0.0270	0.0561	0 0498	0.0378	0.0275
-0.1	0.1018	0.0343	-0.0030	-0.0126	0 0875	0.0520	0.0241	0.0125	0.0772	0.0526	0.0311	0 0206	0.0628	0.0470	0.0322	0.0238
-0.05	0.1039	0.0049	-0 0071	-0.0086	0.0926	0.0343	0.0185	0.0129	0.0831	0.0411	0.0267	0.0205	0 0689	0.0411	0 0296	0.0238
-0.02	0.1052	-0.0027	-0 0038	-0.0038	0.0982	0.0260	0.0192	0.0157	0.0902	0.0351	0.0270	0.0224	0.0765	0.0376	0.0298	0.0249
0.0	±0.1061	0.0	0.0	0 0	-	0.0266	0.0217	0.0185	-	0.0353	0 0289	0 0246	-	0.0378	0.0309	0.0264
0.02	-0.1052	+0.0027	+0 0038	+0 0038	-0.1059	0.0313	0.0256	0 0220	-0.1068	0.0397	0.0320	0.0274	-0.1094	0.0409	0 0330	0.0279
0 05	-0.1039	-0.0049	+0 0071	+0.0086	-0.1097	0 0337	0.0319	0.0277	-0.1121	0 0470	0.0383	0.0325	-0.1157	0.0492	0.0378	0.0320
0.1	-0 1018	-0.0343	+0.0030	0.0126	-0.1111	0.0090	0.0369	0.0366	-0.1154	0.0367	0.0477	0.0421	-0.1202	0.0555	0.0476	0.0398
0.2	-0.0979	-0.0682	-0.0235	0 0036	-0.1107	-0.0481	0.0168	0.0398	-0.1167	-0.0219	0.0423	0.0540	-0.1232	0 0206	0.0584	0.0556
0 3	-0 0944	-0.0783	-0.0446	-0.0136	-0 1090	-0.0736	-0.0139	0.0252	-0.1161	-0.0592	0.0151	0.0490	-0.1238	-0 0237	0.0490	0.0632
0.4	-0.0914	-0.0811	-0 0563	-0.0283	-0.1071	-0.0845	-0.0372	0.0054	-0.1151	-0.0778	-0.0122	0 0334	-0.1237	-0.0537	0.0283	0.0606
0.5	-0.0886	-0.0813	-0 0625	-0.0385	-0.1053	-0.0894	-0.0522	-0.0122	-0.1138	-0.0876	-0.0331	0.0152	-0.1230	-0.0722	0.0060	0.0564
0.6	-0.0861	-0.0805	-0.0656	-0.0453	-0.1034	-0.0914	-0.0617	-0.0260	-0.1125	-0 0928	-0.0479	-0.0015	-0 1221	-0 0836	-0.0135	0.0419
0 7	-0.0836	-0.0792	-0.0670	-0.0496	-0.1014	-0.0921	-0.0677	-0.0362	-0.1110	-0 0957	-0.0583	-0.0155	-0.1210	-0.0909	-0.0294	0.0264
0 8	-0.0812	-0.0776	-0.0673	-0.0522	-0.0995	-0.0919	-0.0714	-0.0437	-0.1094	-0.0970	-0.0655	-0 0267	-0 1200	-0.0956	-0 0420	0.0118
0.9	-0.0790	-0.0758	-0 0670	-0.0537	-0.0976	-0.0912	-0.0737	-0.0492	-0.1078	-0.0975	-0.0705	-0 0354	-0.1190	-0.0988	-0.0518	-0.0012
1 0	-0.0768	-0.0741	-0 0663	-0.0545	-0.0957	-0.0902	-0.0750	-0.0531	-0.1062	-0.0974	-0.0739	-0 0423	-0.1179	-0.1008	-0.0594	-0.0125
1.25	-0.0717	-0.0696	-0.0637	-0.0545	-0.0910	-0.0870	-0.0757	-0.0586	-0.1020	-0.0958	-0.0784	-0.0534	-0.1149	-0.1029	-0.0718	-0.0336
1.5	-0.0670	-0.0654	-0.0606	-0.0530	-0.0864	-0.0834	-0.0744	-0.0605	-0.0980	-0.0932	-0.0795	-0 0592	-0.1117	-0 1026	-0 0783	-0.0470
1 75	-0.0628	-0.0614	-0.0574	-0 0509	-0.0825	-0.0797	-0.0722	-0.0606	-0.0940	-0.0901	-0.0789	-0.0619	-0.1084	-0.1012	-0.0815	-0.0554
2	-0.0589	-0.0577	-0.0542	-0.0485	-0.0782	-0.0766	-0.0696	-0.0596	-0.0901	-0 0868	-0.0774	-0.0628	-0.1050	-0 0991	-0.0826	-0.0603
2.5	-0.0522	-0.0512	-0.0484	-0 0438	-0.0708	-0 0691	-0.0641	-0.0562	-0.0828	-0.0804	-0.0732	-0.0618	-0.0985	-0.0942	-0.0819	-0.0645
3	-0.0466	-0.0458	-0.0434	-0.0395	-0 0646	-0.0630	-0.0589	-0.0524	-0.0763	-0.0743	-0.0685	-0.0597	-0.0923	-0.0889	-0.0791	-0.0648
3.5	-0.0418	-0.0411	-0.0391	-0 0357	-0.0587	-0 0576	-0 0542	-0.0485	-0.0705	-0.0688	-0.0639	-0.0561	-0 0867	-0.0839	-0.0758	-0.0636
4	-0.0378	-0.0372	-0.0354	-0 0324	-0.0540	-0.0529	-0.0499	-0.0450	-0.0654	-0.0639	-0.0597	-0 0528	-0.0816	-0 0792	-0.0723	-0.0617
4 5	-0.0343	-0.0338	-0.0322	-0.0295	-0 0497	-0.0488	-0.0461	-0.0417	-0.0609	-0.0596	-0.0558	-0.0498	-0.0769	-0 0748	-0.0688	-0.0593
5	-0.0314	-0.0309	-0 0294	-0.0271	-0 0460	-0.0452	-0.0428	-0.0388	-0.0568	-0.0557	-0.0523	-0.0468	-0 0726	-0 0708	-0.0655	-0 0570
6	-0.0266	-0.0262	-0.0250	-0.0230	-0.0397	-0 0391	-0.0371	-0.0338	-0.0499	-0.0489	-0.0461	-0.0416	-0.0651	-0.0636	-0.0593	-0.0523
8	-0.0201	-0.0198	-0 0189	-0.0174	-0.0311	-0.0307	-0 0290	-0.0265	-0.0397	-0.0390	-0.0369	-0.0335	-0.0535	-0.0524	-0.0493	-0.0441
10	-0 0161	-0.0158	-0.0151	-0.0140	-0.0253	-0 0249	-0.0237	-0.0217	-0.0328	-0.0323	-0.0306	-0.0279	-0 0452	-0.0444	-0.0418	-0.0377
20	-0.0080	-0 0079	-0.0075	-0.0069	-0.0131	-0.0129	-0 0123	-0.0113	-0.0176	-0.0173	-0.0165	-0.0151	-0.0255	-0.0251	-0.0238	-0.0217

SYMBOLS

c	wing chord
C_L	lift coefficient
$\ell(x,y)$	strength of the distribution of lifting singularities
$q(x,\theta)$	strength of source distribution on the fuselage related to a single vortex with triple kink
$q^{(0)}(x,\theta)$	first approximation to $q(x,\theta)$, see equation (6)
$q^{(1)}(x,\theta)$	second approximation to $q(x,\theta)$, see equations (7) to (9)
R	radius of fuselage
t/c	thickness-to-chord ratio
V_0	free stream velocity, taken as unity
$\underline{v}$	perturbation velocity
$\underline{v}_{\wedge\wedge}$	velocity induced by single vortex with three kinks, see equation (A-1)
$\underline{v}_{\Lambda}$	velocity induced by single vortex with one kink, see equation (B-1)
$\underline{v}_q$	velocity induced by source distribution $q(x,\theta)$ on fuselage
$\underline{v}_I$	$= \underline{v}_q + \underline{v}_{\wedge\wedge} - \underline{v}_{\Lambda}$, interference velocity related to single vortex
v_n	velocity component normal to the surface of the fuselage
$v_{n\Gamma}$	normal velocity induced by single vortex with three kinks $= v_{n\wedge\wedge}$
v_x, v_y, v_z	components of perturbation velocity with respect to the various axes
$v_{x\ell}$, $v_{y\ell}$, $v_{z\ell}$	velocity components for the isolated wing induced by the load distribution $\ell(x,y)$
v_{xt}, v_{yt}, v_{zt}	velocity components for the isolated wing induced by the source distribution in the wing plane
$\Delta\underline{v}$	difference between the velocity field past the wing-fuselage combination and the velocity field past the wing attached to an infinite reflection plate
$-\Delta v_{zJ}$	interference downwash in the wing-body junction
x, y, z	rectangular coordinate system, x-axis coincides with the axis of the fuselage
x, r, θ	system of cylindrical coordinates
$x_{TE}(y)$	ordinate of trailing edge
$z_s(x,y)$	camber distribution of isolated wing
$2z_t(x,y)$	thickness distribution
$\Delta z(x,y)$	$= \Delta z_s(x,y) + \Delta\alpha(y)(x_{TE} - x)$, change in wing warp produced by the body interference
$\Delta z^{(1)}$	additional wing warp from first-order theory

SYMBOLS (concluded)

$\Delta z^{(2)}$	additional wing warp from second-order theory
$\Delta z_s(x,y)$	additional camber produced by the body interference
$\alpha(y)$	twist distribution of isolated wing
$\Delta\alpha(y)$	additional twist produced by the body interference
Γ	strength of isolated vortex
$\gamma(\xi)$	strength of vorticity distribution
$\theta_J(x)$	$= \sin^{-1}\left(\frac{c}{R}\frac{z_t(x)}{c}\right)$
ξ	$= x - (\lvert y\rvert - R)\tan\phi$
ϕ	angle of sweep

REFERENCES

No.	Author	Title, etc.
1	J. Weber	Interference problems on wing-fuselage combinations. Part I: Lifting unswept wing attached to a cylindrical fuselage at zero incidence in midwing position. RAE Technical Report 69130 (ARC 31532) (1969)
2	J. Weber M.G. Joyce	Interference problems on wing-fuselage combinations. Part II: Symmetrical unswept wing at zero incidence attached to a cylindrical fuselage at zero incidence in midwing position. RAE Technical Report 71179 (ARC 33437) (1971)
3	J. Weber M. Gaynor Joyce	Interference problems on wing-fuselage combinations. Part III: Symmetrical swept wing at zero incidence attached to a cylindrical fuselage. RAE Technical Report 73189 (ARC 35413) (1974)
4	H. Kramer	Some analytical and numerical calculations for a cylinder-vortex combination in incompressible flow. NLR - TR 69057 U (1969)
5	J. Weber	Second-order small-perturbation theory for finite wings in incompressible flow. ARC R & M 3759 (1972)
6		Method for predicting the pressure distribution on swept wings with subsonic attached flow. Roy. Aero. Soc. Trans. Data Memo. 6312 (1963) (Revised version to be issued as TDM 73012)
7	J.L. Hess A.M.O. Smith	Calculation of potential flow about arbitrary bodies. Progress in Aeron. Scs., Vol.8 (1967)
8	A. Roberts K. Rundle	The computation of first order compressible flow about wing-body configurations. BAC, Weybridge Ma Report 20 (1973)

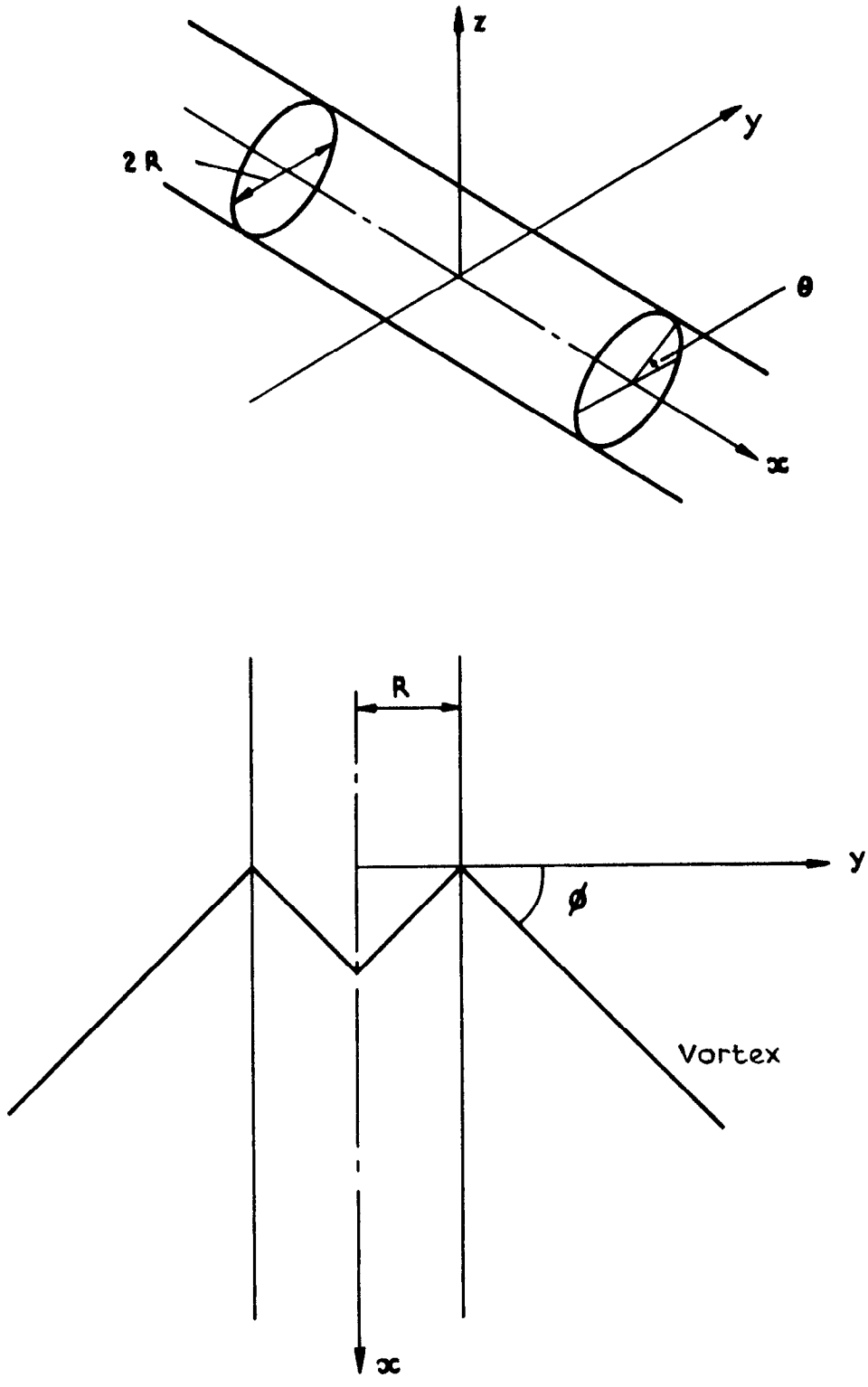

Fig. 1 Notation

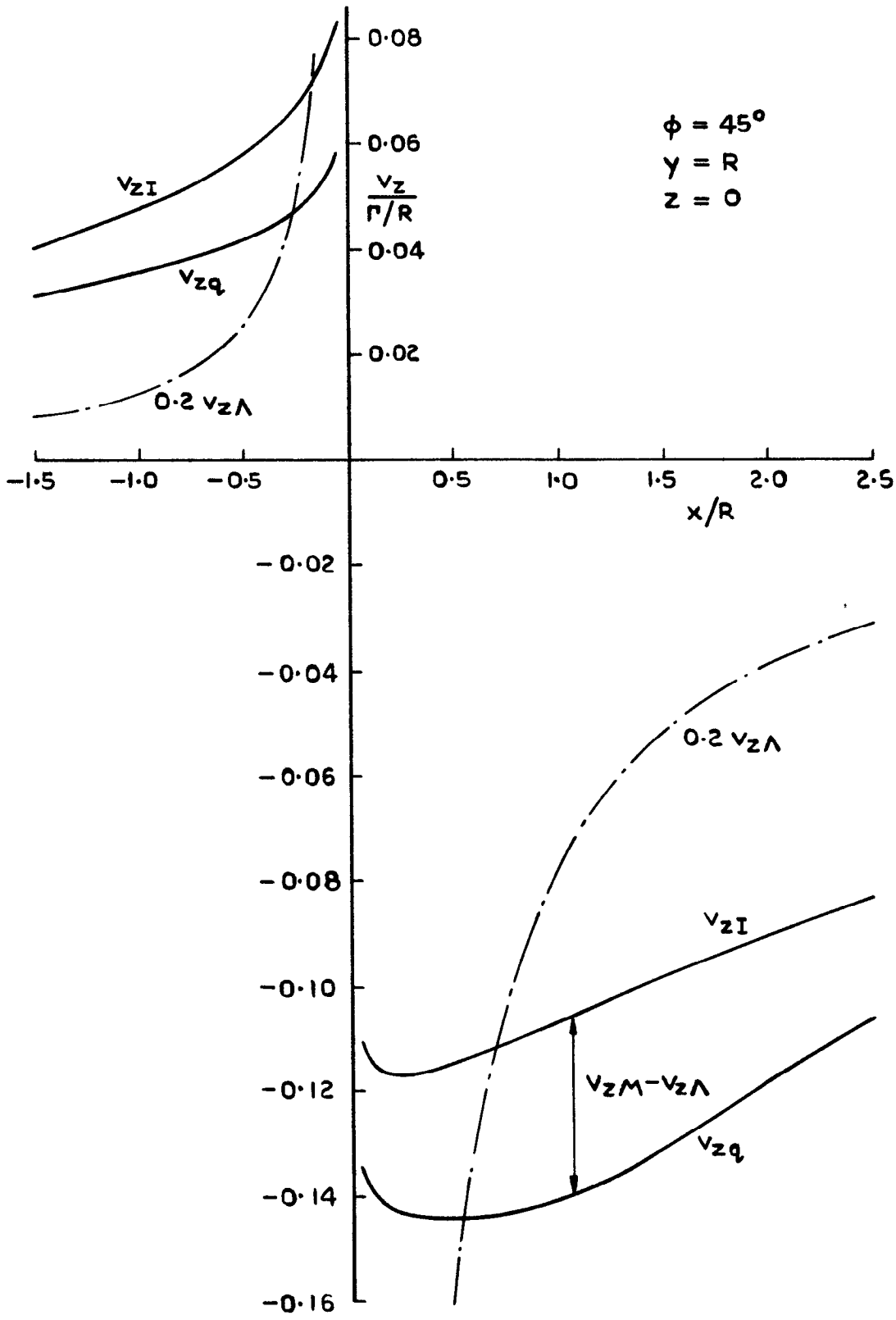

Fig.2 Additional downwash in the wing-body junction

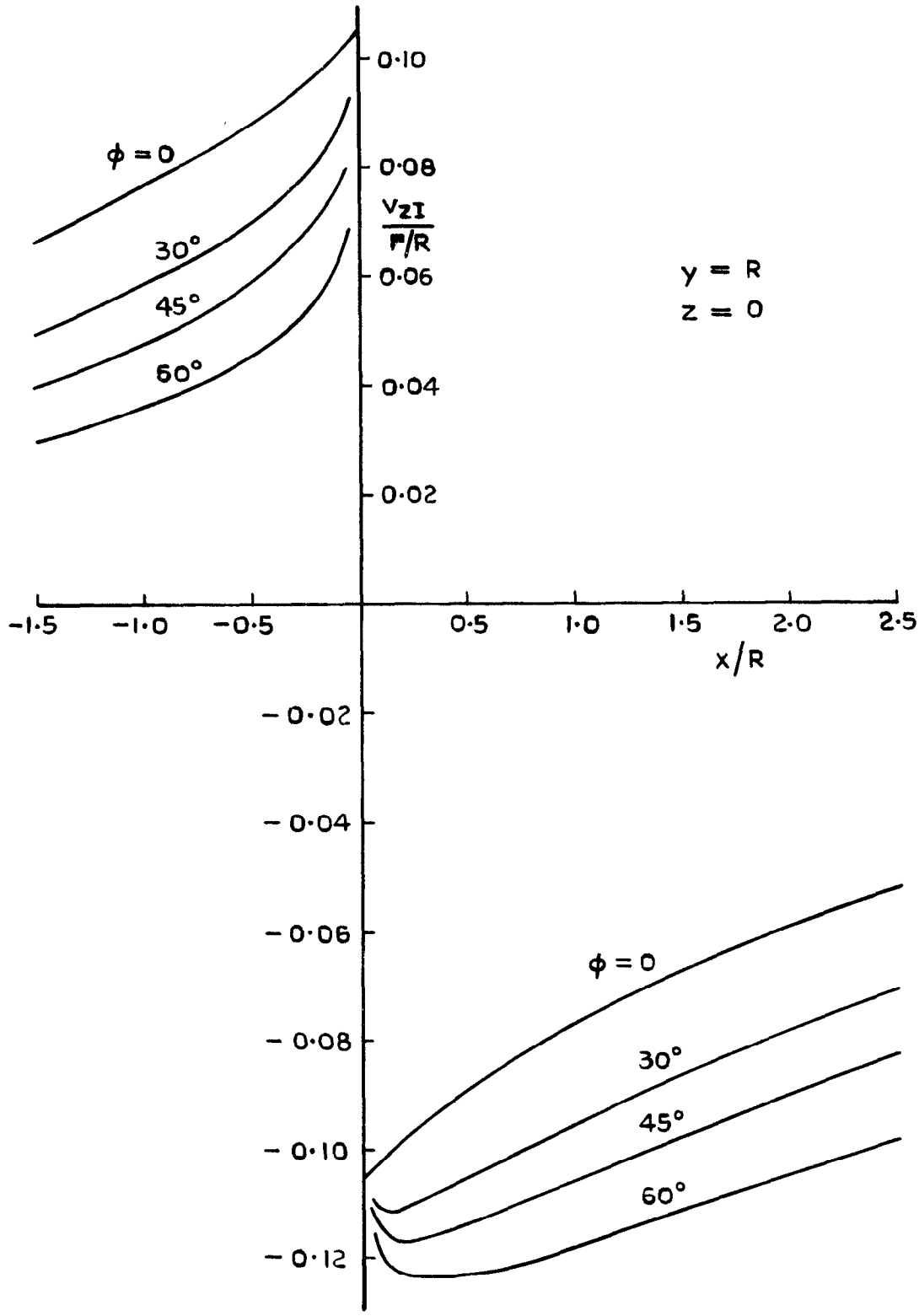

Fig.3 Additional downwash in the wing-body junction

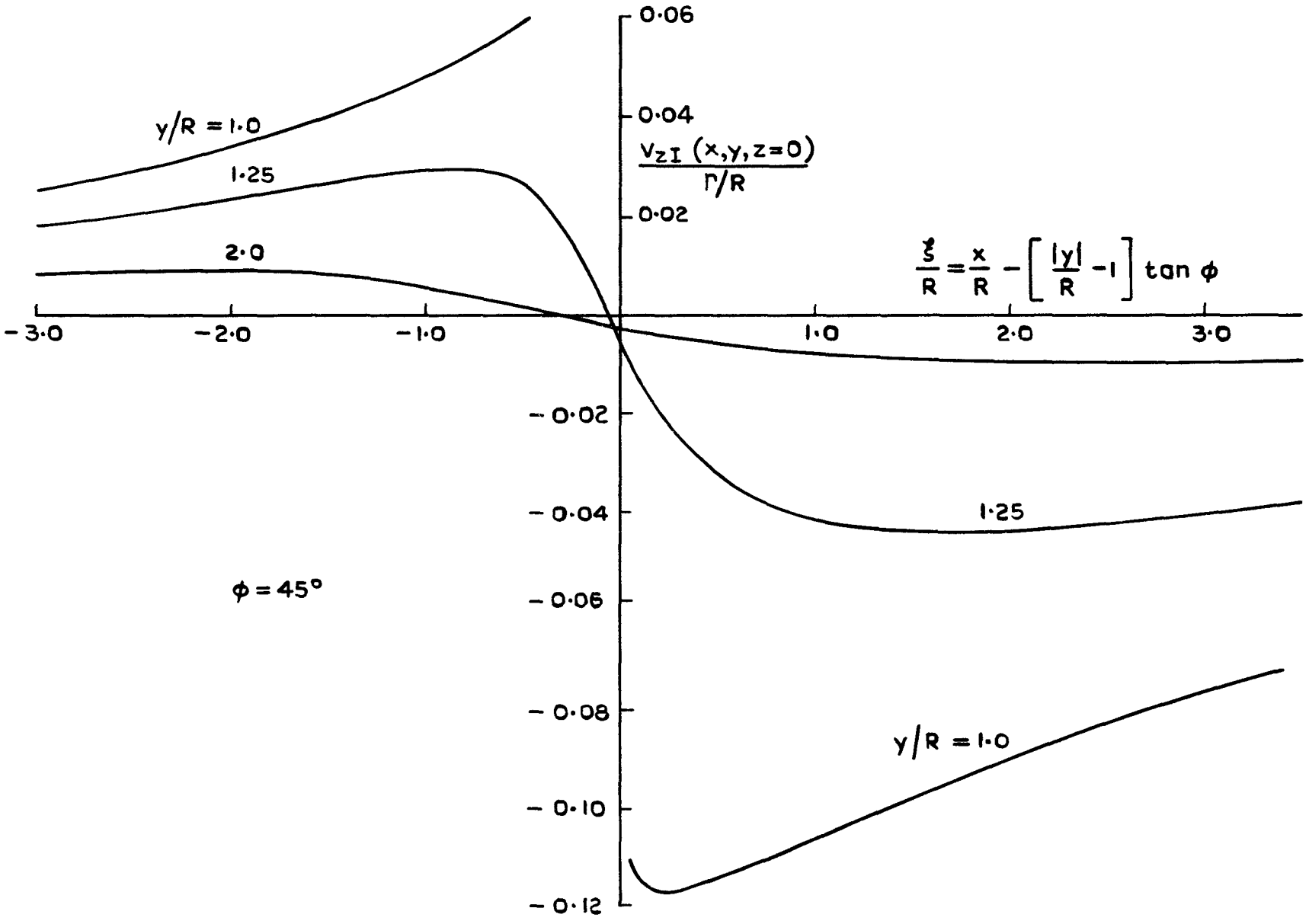

Fig.4 Additional downwash in the plane z=O

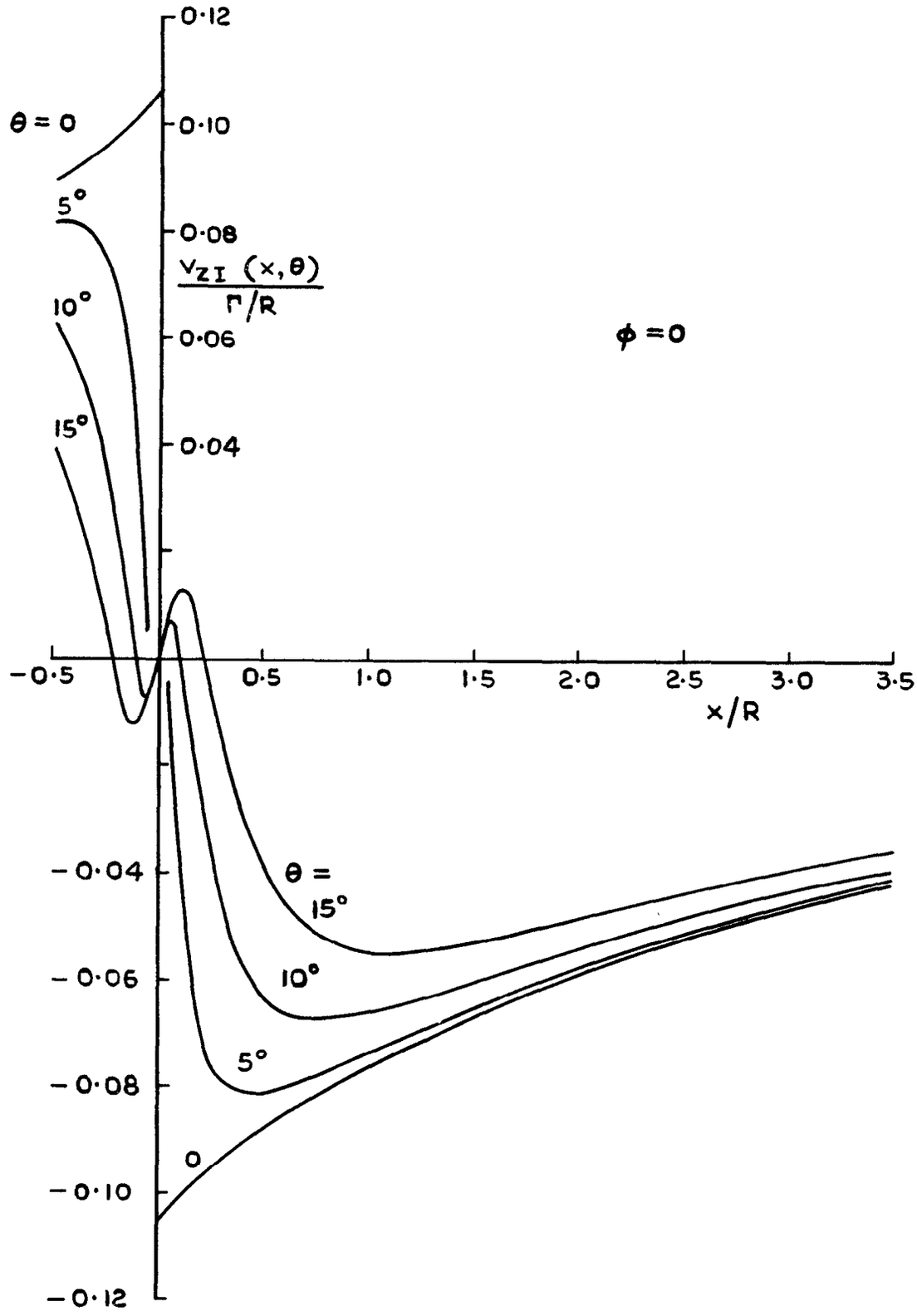

Fig.5 Additional downwash on the fuselage

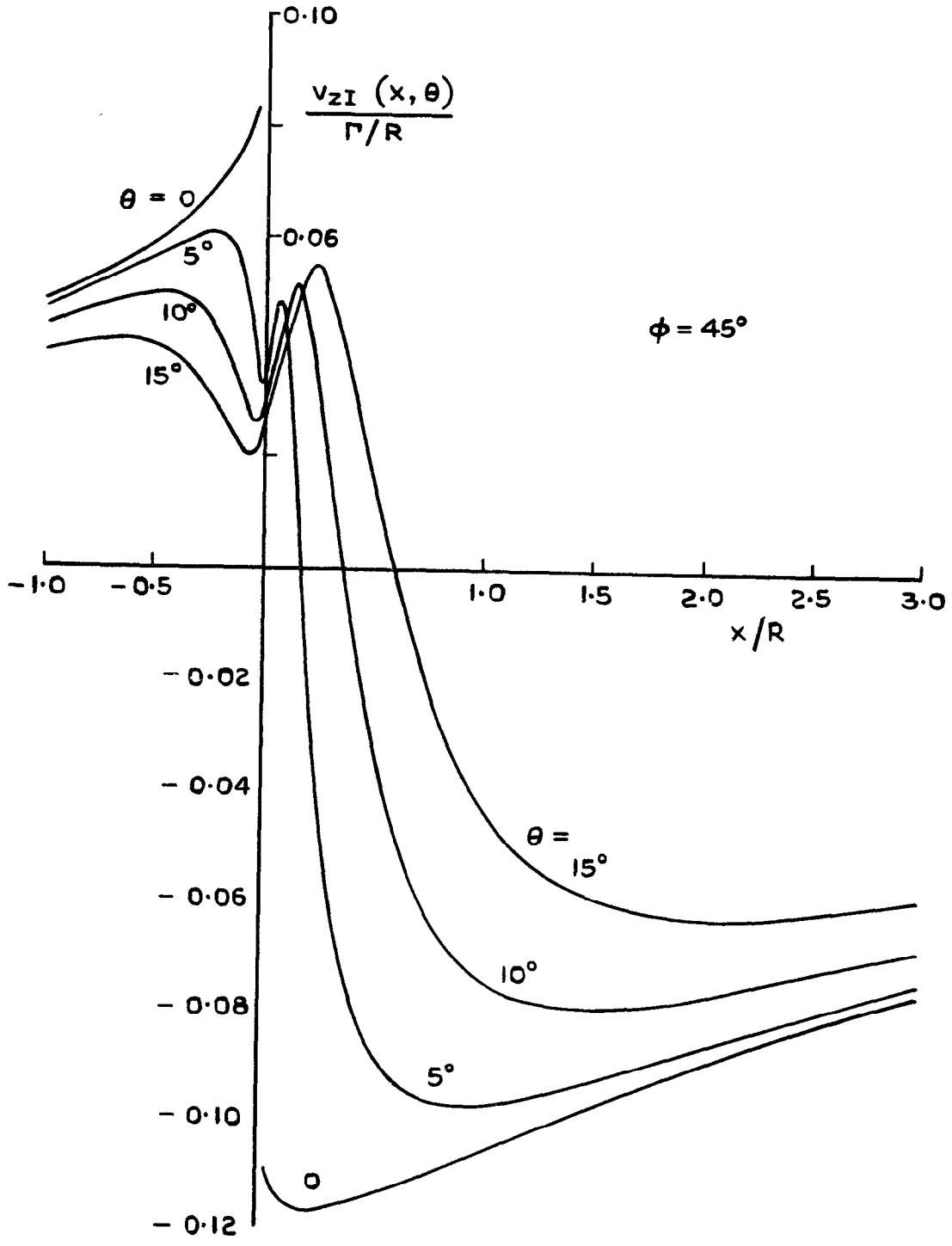

Fig.6 Additional downwash on the fuselage

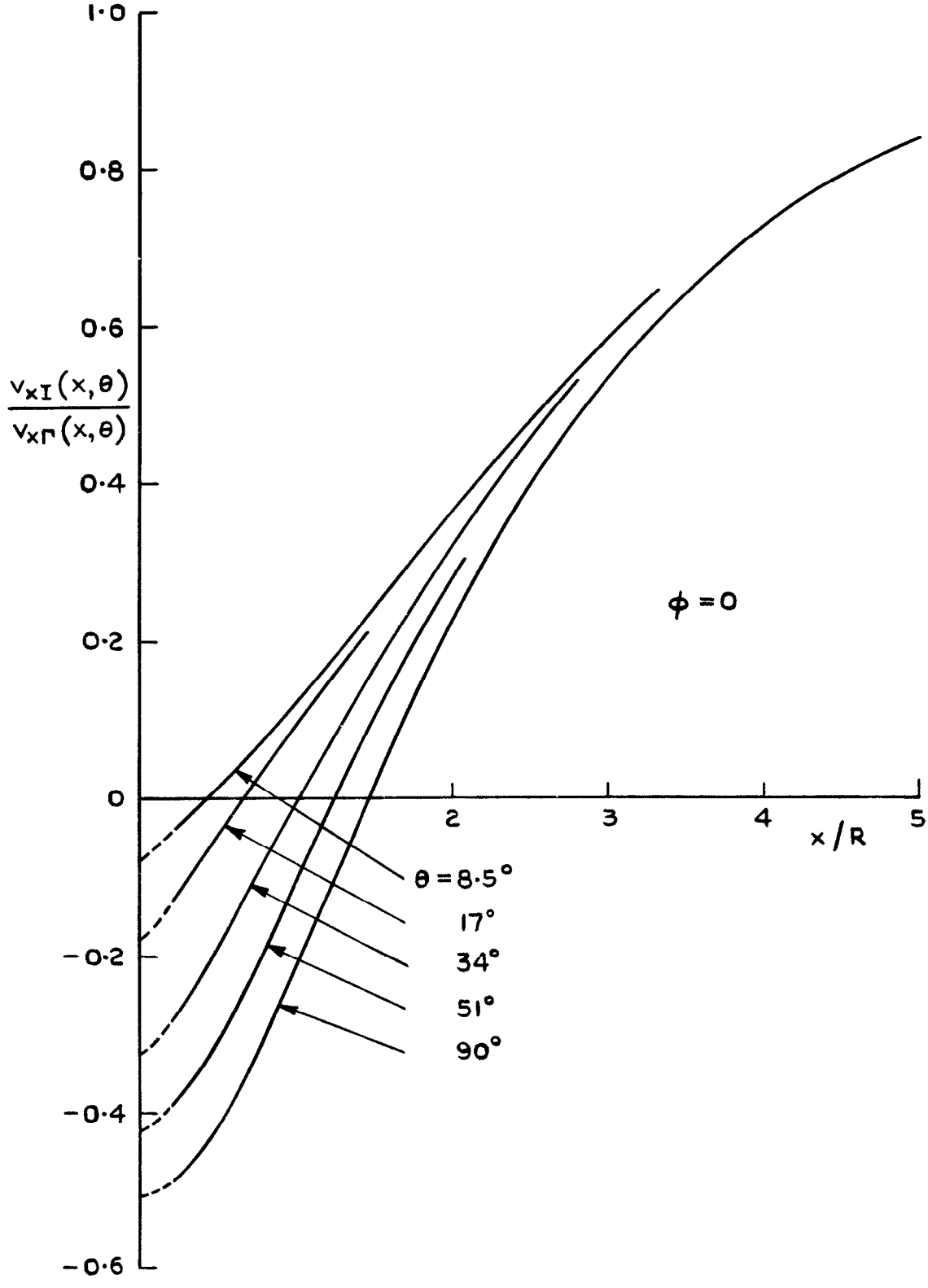

Fig.7 Additional streamwise velocity on the fuselage

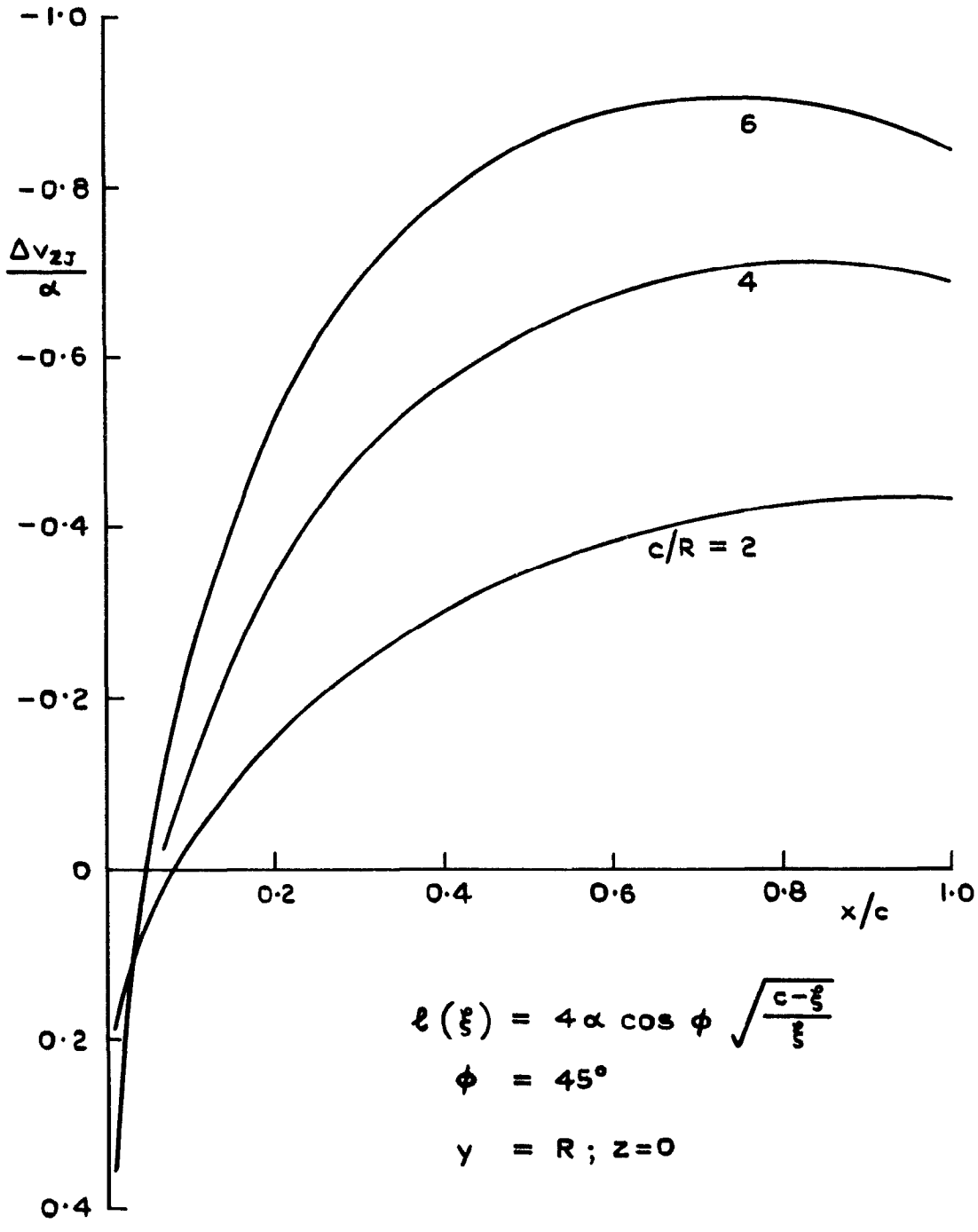

Fig. 8 Additional downwash in the wing–body junction

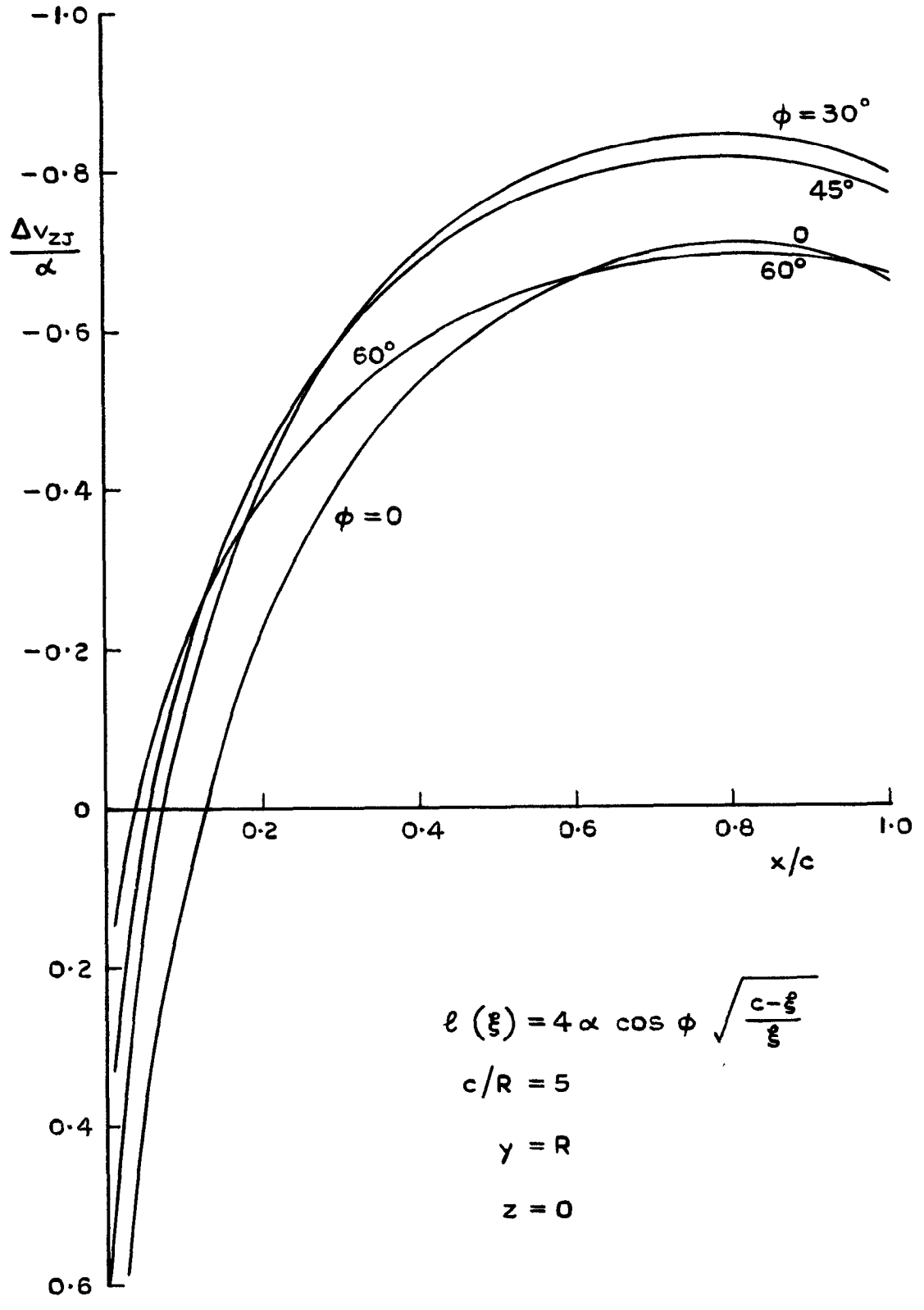

Fig.9 Additional downwash in the wing-body junction

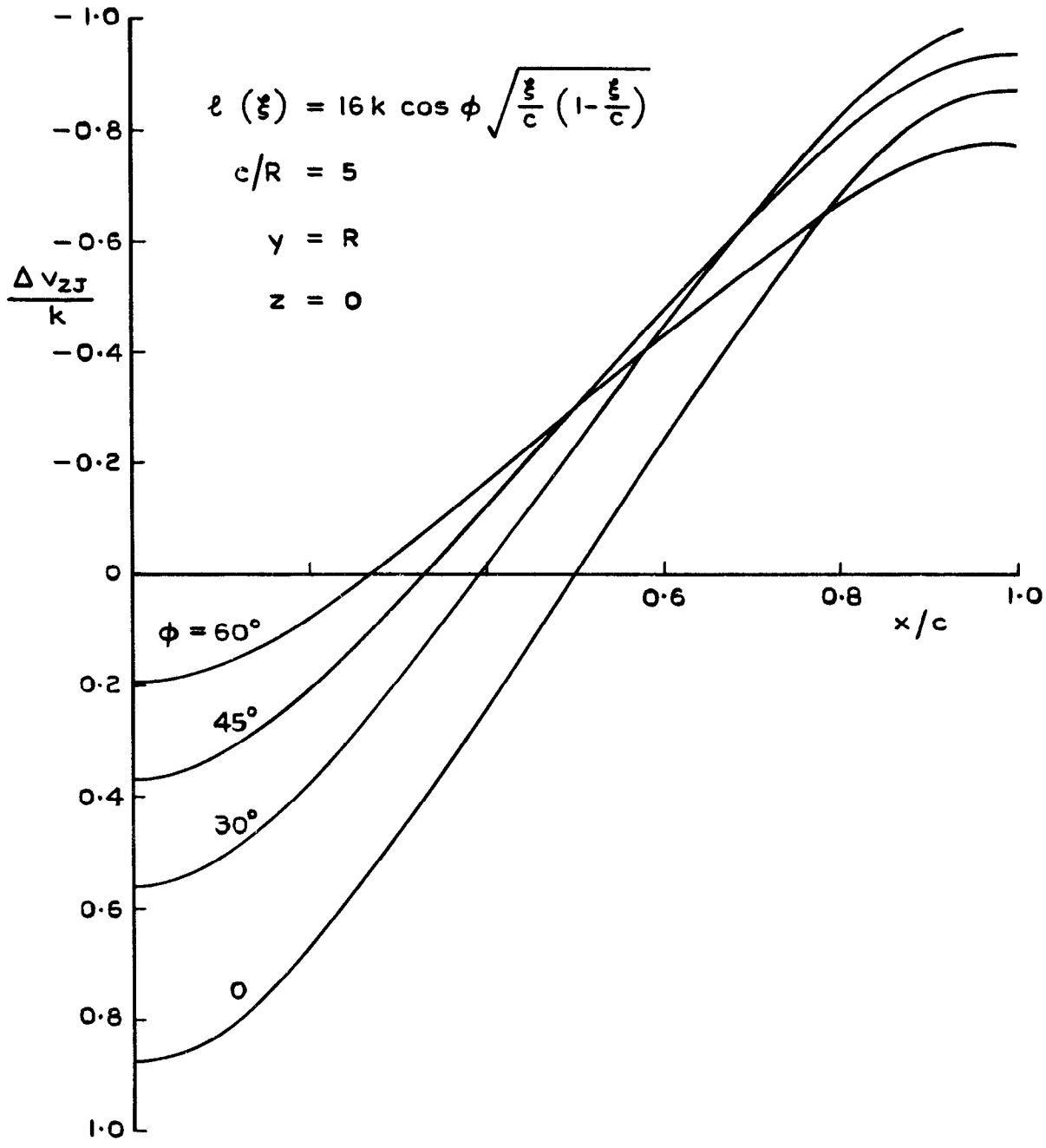

Fig.10 Additional downwash in the wing-body junction

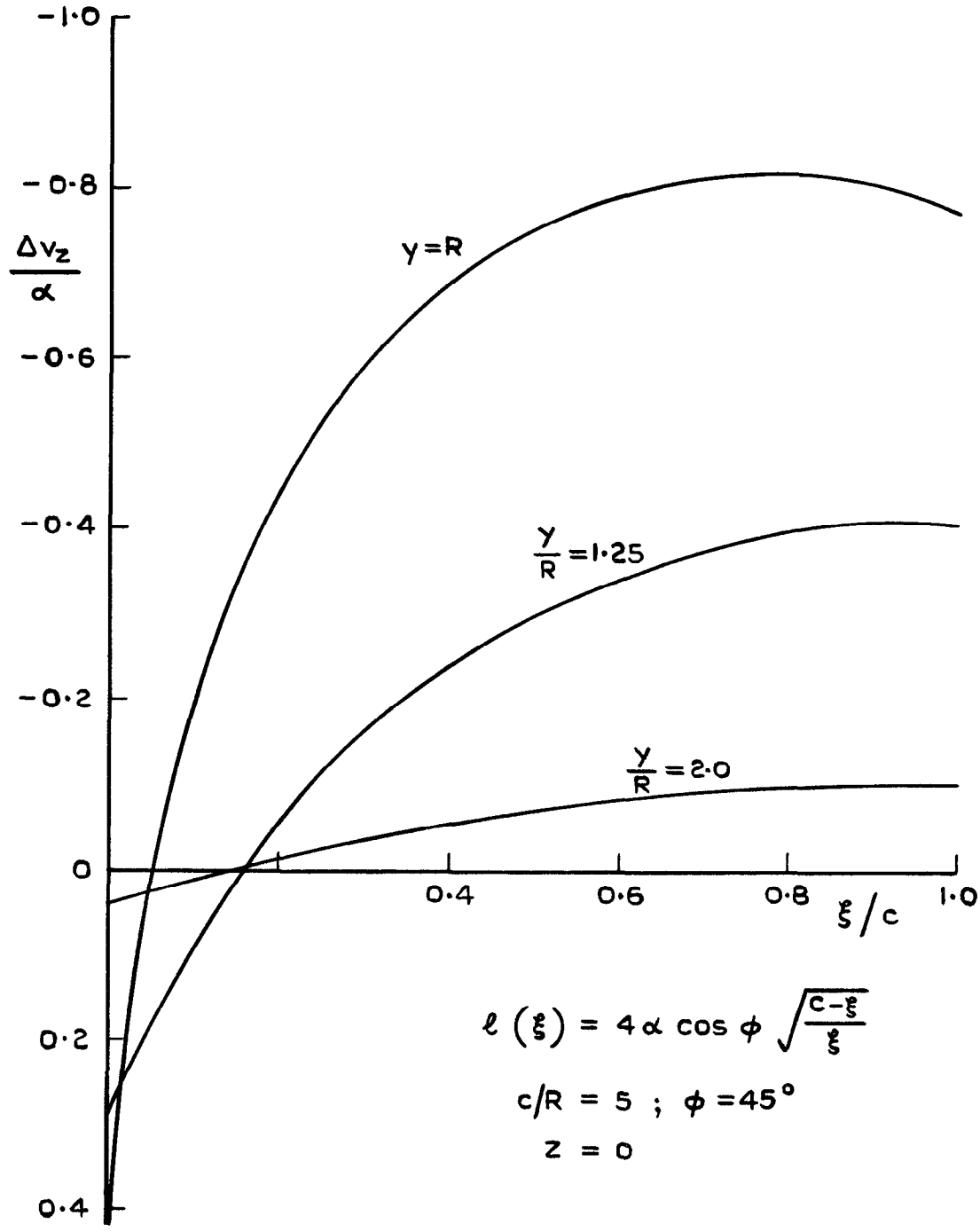

Fig. 11 Additional downwash in the wing plane

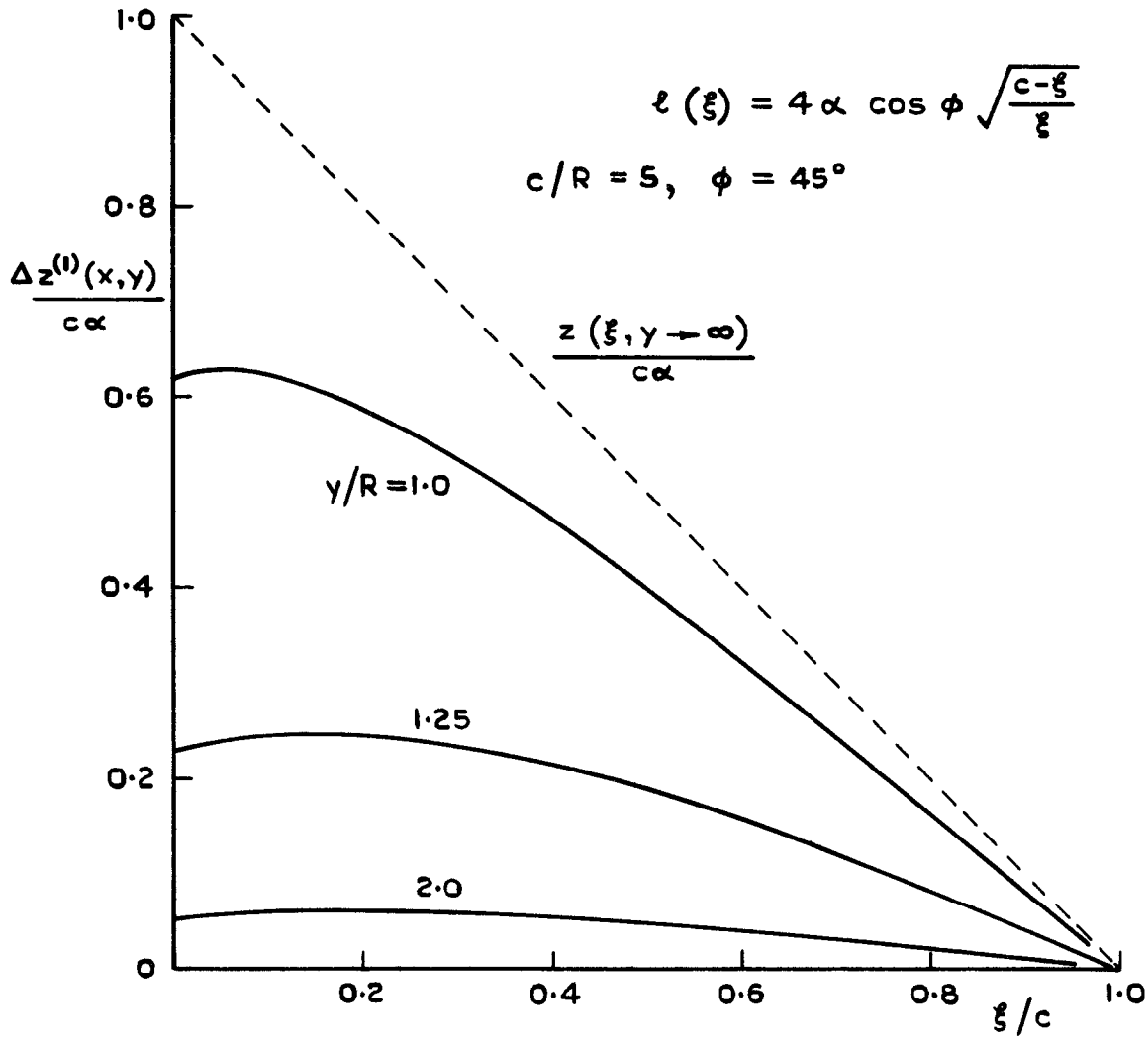

Fig. 12 Additional wing warp

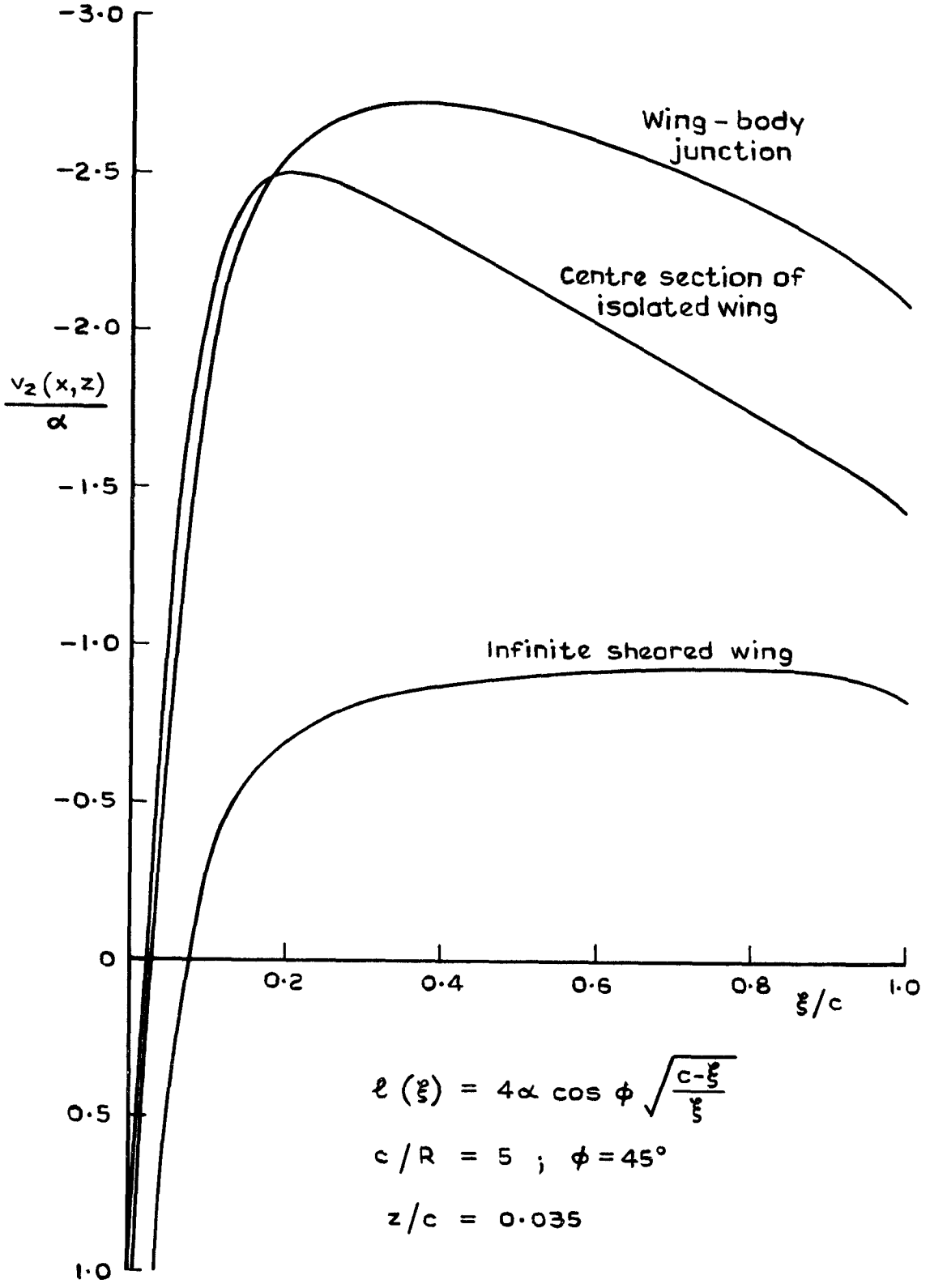

Fig.13 Downwash distributions at various spanwise stations

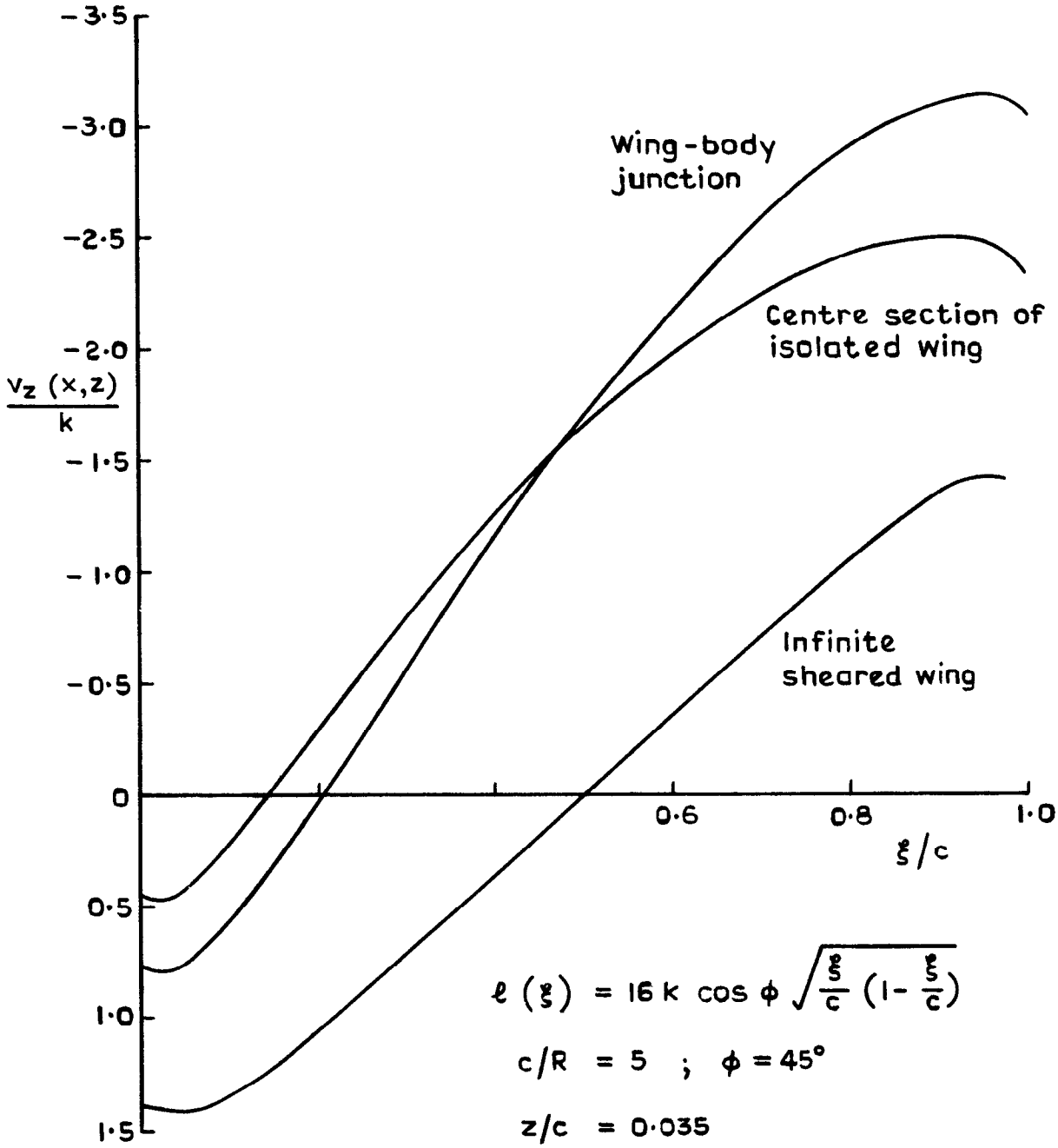

Fig 14 Downwash distributions at various spanwise stations

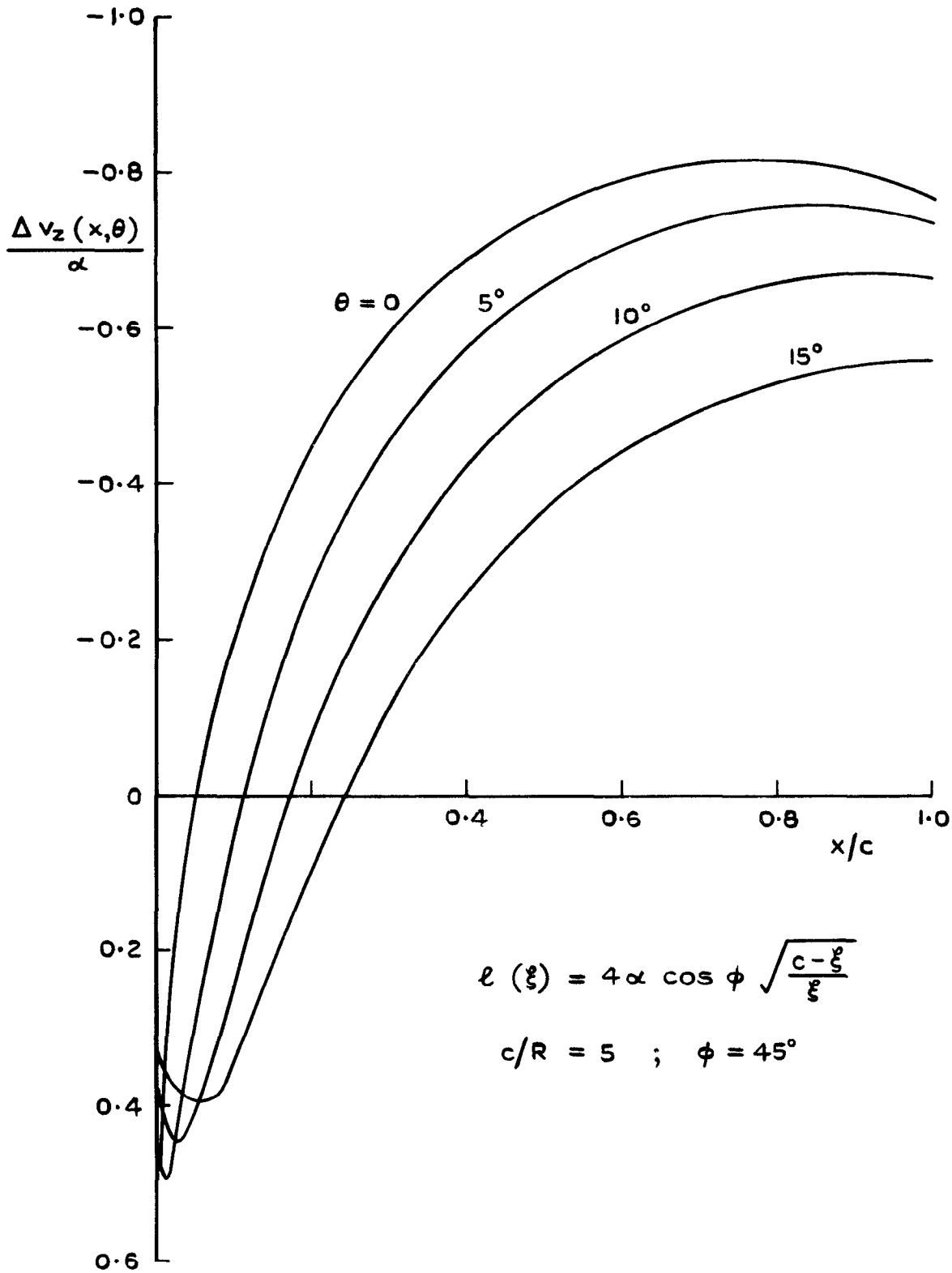

Fig.15 Downwash distributions in the wing-body junction

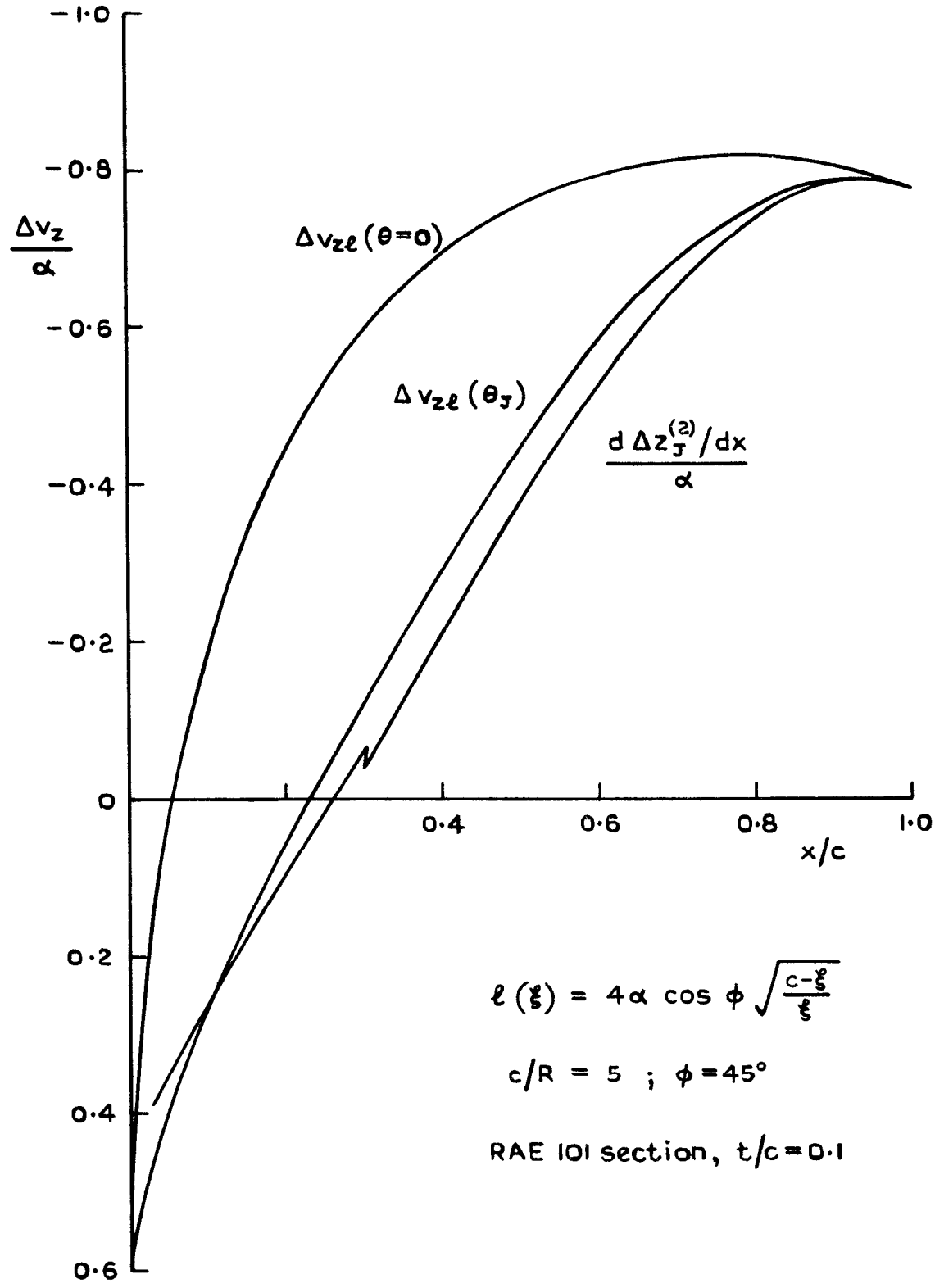

Fig.16 Downwash distributions in the wing-body junction

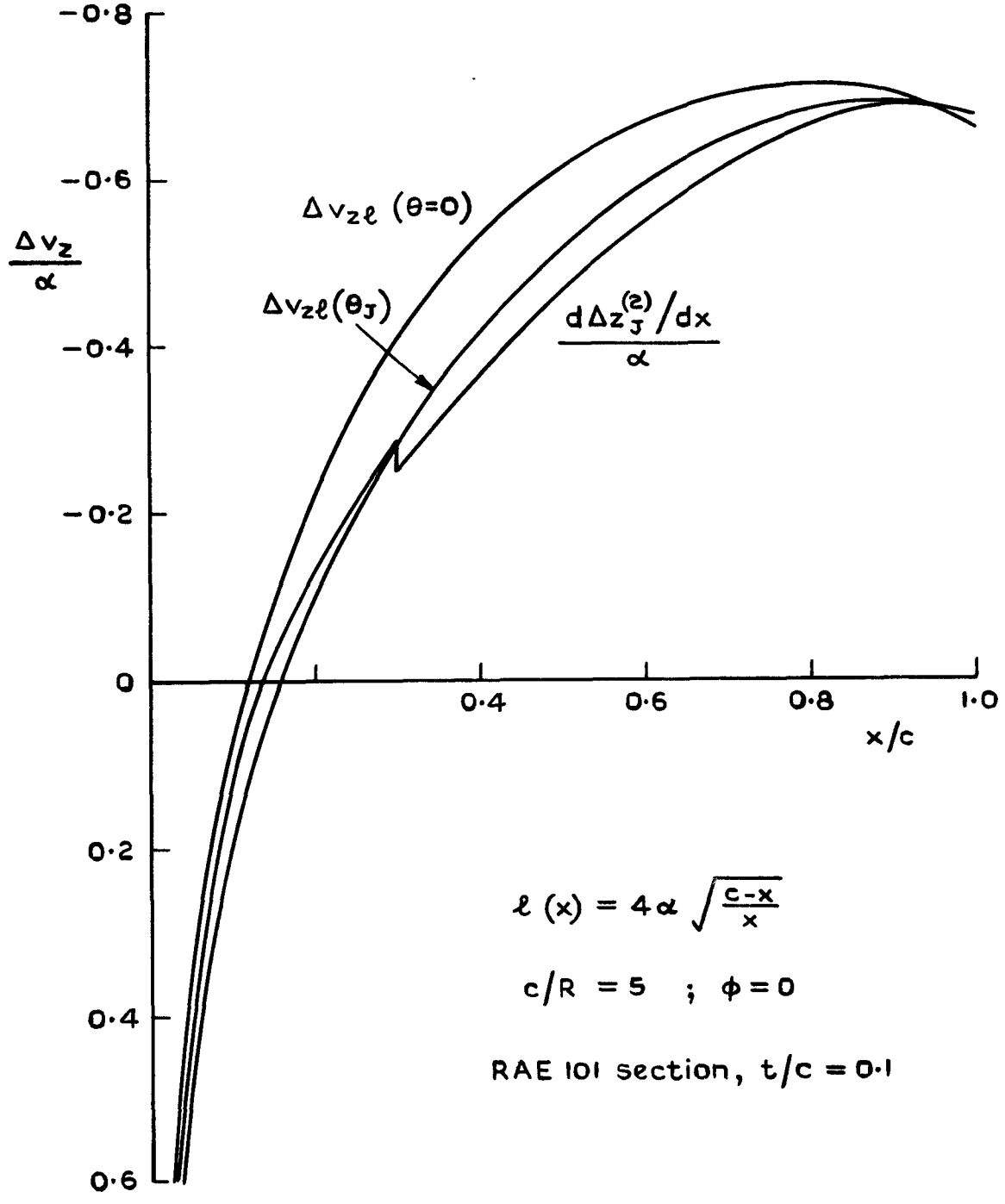

Fig.17 Downwash distributions in the wing-body junction

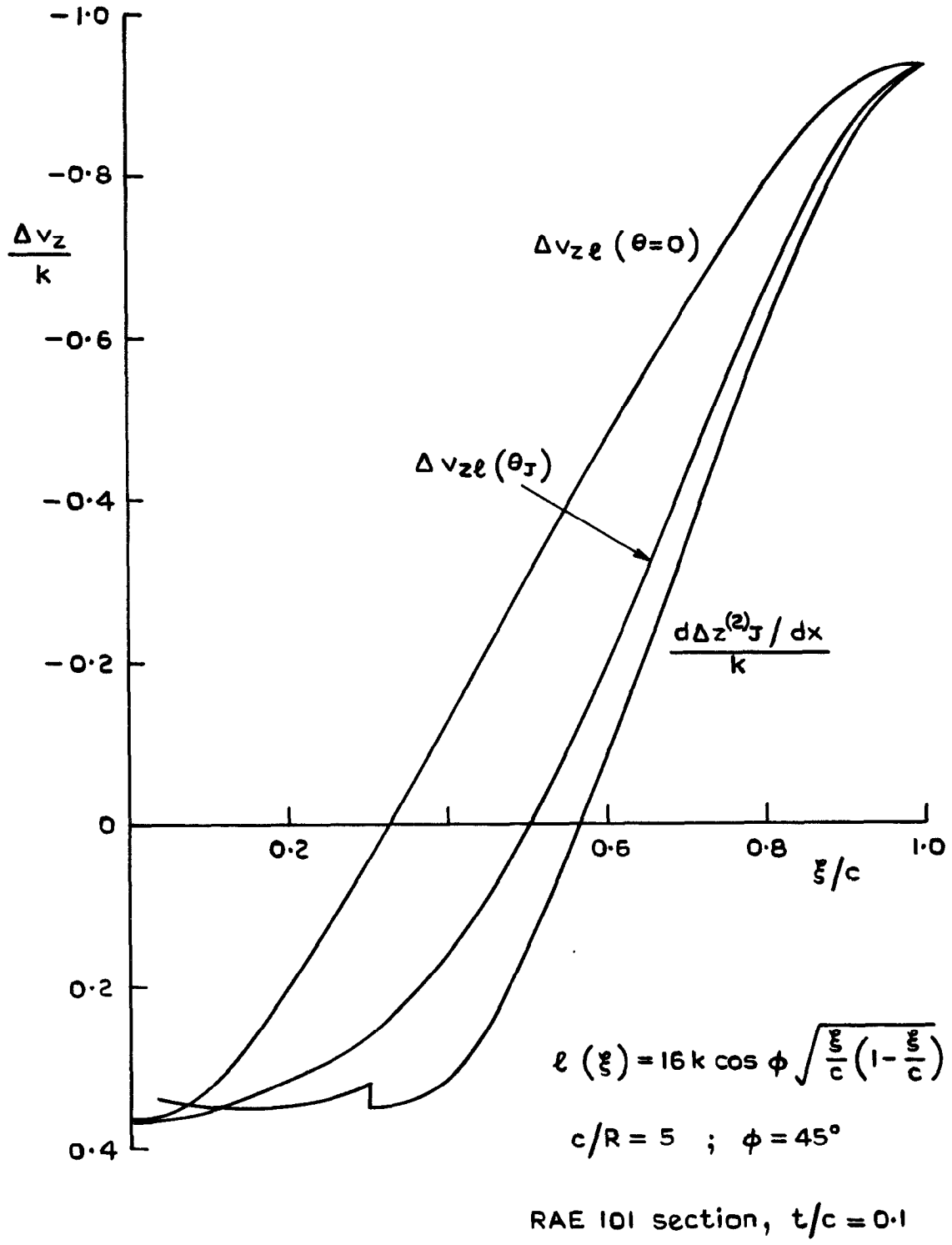

Fig.18 Downwash distributions in the wing-body junction

Printed in England for Her Majesty's Stationery Office by the Royal Aircraft Establishment, Farnborough Dd 289030 K5 10/75

ARC CP No.1334
December 1973

Weber, J.
Joyce, M. Gaynor

533.695.12 :
533.693.1 :
533.6.048.1 :
533.6.048.3 :
533.6.04 .
533.6.011.32

INTERFERENCE PROBLEMS ON WING-FUSELAGE COMBINATIONS. PART IV THE DESIGN PROBLEM FOR A LIFTING SWEPT WING ATTACHED TO A CYLINDRICAL FUSELAGE

The incompressible flow field past a circular cylindrical fuselage and a kinked infinite swept vortex, which lies in a plane through the axis of the fuselage, has been studied. In particular values for the downwash in this plane and on the surface of the fuselage have been determined numerically; the values are tabulated for four angles of sweep: 0, 30°, 45°, 60°.

The results are used to design wings of constant chord and infinite aspect ratio, attached to a cylindrical fuselage in midwing position, for which the chordwise load distribution is given and the spanwise distribution in the presence of the fuselage is required to be constant. It is shown how the interference effect varies with the angle of sweep, with the ratio R/c between the body radius and the wing chord, with the spanwise distance from the wing-body junction and with the thickness of the wing.

ARC CP No.1334
December 1973

Weber, J.
Joyce, M. Gaynor

533.695.12 :
533.693.1 .
533.6.048.1 :
533.6.048.3 :
533.6.04 :
533.6.011.32

INTERFERENCE PROBLEMS ON WING-FUSELAGE COMBINATIONS. PART IV THE DESIGN PROBLEM FOR A LIFTING SWEPT WING ATTACHED TO A CYLINDRICAL FUSELAGE

The incompressible flow field past a circular cylindrical fuselage and a kinked infinite swept vortex, which lies in a plane through the axis of the fuselage, has been studied. In particular values for the downwash in this plane and on the surface of the fuselage have been determined numerically; the values are tabulated for four angles of sweep: 0, 30°, 45°, 60°.

The results are used to design wings of constant chord and infinite aspect ratio, attached to a cylindrical fuselage in midwing position, for which the chordwise load distribution is given and the spanwise distribution in the presence of the fuselage is required to be constant. It is shown how the interference effect varies with the angle of sweep, with the ratio R/c between the body radius and the wing chord, with the spanwise distance from the wing-body junction and with the thickness of the wing.

Cut here

ARC CP No.1334
December 1973

Weber, J.
Joyce, M. Gaynor

533.695.12 :
533.693.1 :
533.6.048.1 :
533.6.048.3 :
533.6.04 :
533.6.011.32

INTERFERENCE PROBLEMS ON WING-FUSELAGE COMBINATIONS. PART IV THE DESIGN PROBLEM FOR A LIFTING SWEPT WING ATTACHED TO A CYLINDRICAL FUSELAGE

The incompressible flow field past a circular cylindrical fuselage and a kinked infinite swept vortex, which lies in a plane through the axis of the fuselage, has been studied. In particular values for the downwash in this plane and on the surface of the fuselage have been determined numerically; the values are tabulated for four angles of sweep: 0, 30°, 45°, 60°.

The results are used to design wings of constant chord and infinite aspect ratio, attached to a cylindrical fuselage in midwing position, for which the chordwise load distribution is given and the spanwise distribution in the presence of the fuselage is required to be constant. It is shown how the interference effect varies with the angle of sweep, with the ratio R/c between the body radius and the wing chord, with the spanwise distance from the wing-body junction and with the thickness of the wing.

Cut here

DETACHABLE ABSTRACT CARDS

DETACHABLE ABSTRACT CARDS

Published by
HER MAJESTY'S STATIONERY OFFICE

Government Bookshops
49 High Holborn, London WC1V 6HB
13a Castle Street, Edinburgh EH2 3AR
41 The Hayes, Cardiff CF1 1JW
Brazennose Street, Manchester M60 8AS
Southey House, Wine Street, Bristol BS1 2BQ
258 Broad Street, Birmingham B1 2HE
80 Chichester Street, Belfast BT1 4JY
Government Publications are also available through booksellers

C.P. No. 1334

ISBN 011 470944 0